

Review

A Review of Low Temperature NH₃-SCR for Removal of NO_x

Devaiah Damma ¹, Padmanabha R. Ettireddy ², Benjaram M. Reddy ³ and Panagiotis G. Smirniotis ^{1,*}

¹ Chemical Engineering, College of Engineering and Applied Science, University of Cincinnati, Cincinnati, OH 45221-0012, USA; dammadh@ucmail.uc.edu

² Cummins Inc., Columbus, IN 47201, USA; ettireddypr@gmail.com

³ Catalysis and Fine Chemicals Department, CSIR-Indian Institute of Chemical Technology (IICT), Uppal Road, Hyderabad, Telangana 500007, India; bmreddy@iiict.res.in

* Correspondence: smirnipp@ucmail.uc.edu; Tel.: +1-513-556-1474; Fax: +1-513-556-3473

Received: 6 March 2019; Accepted: 4 April 2019; Published: 10 April 2019



Abstract: The importance of the low-temperature selective catalytic reduction (LT-SCR) of NO_x by NH₃ is increasing due to the recent severe pollution regulations being imposed around the world. Supported and mixed transition metal oxides have been widely investigated for LT-SCR technology. However, these catalytic materials have some drawbacks, especially in terms of catalyst poisoning by H₂O or/and SO₂. Hence, the development of catalysts for the LT-SCR process is still under active investigation throughout seeking better performance. Extensive research efforts have been made to develop new advanced materials for this technology. This article critically reviews the recent research progress on supported transition and mixed transition metal oxide catalysts for the LT-SCR reaction. The review covered the description of the influence of operating conditions and promoters on the LT-SCR performance. The reaction mechanism, reaction intermediates, and active sites are also discussed in detail using isotopic labelling and in situ FT-IR studies.

Keywords: low-temperature selective catalytic reduction; NH₃-SCR; de-NO_x catalysis; SO₂/H₂O tolerance; transition metal-based catalysts

1. Introduction

The non-renewable fossil fuels are continuing to remain the dominant energy source in power plants and automobiles to satisfy the ever-growing energy demands. However, the combustion of fossil fuels mainly generates nitrogen oxide (NO_x) pollutants (NO, NO₂, and N₂O and their derivatives) which can cause acid rain, photochemical smog, ozone depletion, and eutrophication problems [1–4]. Due to the negative impacts of NO_x, the mitigation of NO_x emissions is of paramount importance for environmental protection. Several technologies are available to reduce NO_x emissions by using catalytic materials and among them, selective catalytic reduction of NO_x with NH₃ (NH₃-SCR) has been widely applied due to its high NO_x removal efficiency [5–7]. Usually, the flue gas temperature of the industrial process is as low as 300 °C and, thus, the SCR catalyst must be active in the low-temperature regime (100–300 °C). V₂O₅–WO₃(MoO₃)/TiO₂ is the typical and efficient catalyst and has been commercialized for NH₃-SCR technology for medium temperature process [8,9]. However, this catalyst has some intrinsic drawbacks such as narrow and high working temperature window (350–400 °C), and low N₂ selectivity in the high-temperature range [3,10,11]. Therefore, many researchers continue to develop highly active catalysts for low-temperature NH₃-SCR in a wide temperature window.

With this perspective, several transition metal oxide-based catalysts have been extensively investigated for low-temperature NH₃-SCR reaction due to their excellent redox properties, low price,

and high thermodynamic stability. Especially, the easy gain and loss of electrons in the *d* shell of the transition metal ions could be responsible for the facile redox properties [12–14]. For example, the Cr/TiO₂ [15], Cr-MnO_x [8], Fe-MnO_x [16], Mn/TiO₂ [17,18], Fe_xTiO_y [19], MnO_x/CeO₂ [20], and Cu/TiO₂ [21] catalysts were shown to exhibit good SCR activity in the low temperature range. In our earlier work, we investigated the low-temperature NH₃-SCR in the presence of excess O₂ on the TiO₂ supported V, Cr, Mn, Fe, Co, Ni, and Cu oxides and found the catalytic performance decreased in the following order of Mn > Cu ≥ Cr ≫ Co > Fe ≫ V ≫ Ni [16]. Particularly, manganese-containing catalysts have attracted much attention due to its variable valence states and excellent redox ability [2,5]. In the recent past, we published a series of papers on Mn-based SCR catalysts that showed a highly promising deNO_x potential in the low-temperature region [5,22–26]. However, these catalysts are very sensitive to the presence of SO₂ in the feed and exhibit lower N₂ selectivity [8,27–29]. Hence, the development of catalysts that show both good low-temperature activity and high SO₂/H₂O durability is of great importance for the NH₃-SCR reaction. In general, there are two plausible strategies available to enhance low-temperature NH₃-SCR performance. One strategy is to modify the transition metal oxide with one or multiple metal oxides, which could enhance the active sites for the reaction by inducing the synergistic effect [30–33]. The other approach is to synthesize the supported materials to disperse the transition metal-based oxides which can increase the activity by metal-support interactions [26,34–37]. Recently, many supported and mixed transition metal catalyst formulations have been studied to improve the low-temperature SCR performance, as well as resistance to SO₂/H₂O.

In this study, we systematically reviewed the recent advancements in developing the transition metal-based catalysts for low-temperature NH₃-SCR reaction. This review also demonstrated the action of different promoters and supports on the catalytic performance and SO₂/H₂O tolerance of the transition metal-based catalysts in NH₃-SCR of NO_x. The reported catalysts were divided into four categories, such as binary, ternary/multi, supported single, and supported binary/multi-transition metal-based catalysts.

2. Binary Transition Metal-Based Catalysts

Various transition-metal oxides have been proved to be active for the NH₃-SCR at low-temperature. However, the catalytic performance on single transition metal oxide is far from satisfactory due to their low specific surface area and thermal instability [38–41]. The addition of dopants is a common method to improve the drawbacks associated with pure transition metal oxide. Hence, much progress has done to improve the low-temperature SCR activity of transition metal oxides by mixing or doping with other metal oxides. In recent years, Mn, Fe, Co, Ni, and Cu-based binary oxide catalysts have been extensively studied for low-temperature NH₃-SCR reaction due to their attractive catalytic performance [19,33,41–49]. Particularly, Mn-based binary oxides are popular and proven to be effective catalysts for low-temperature NH₃-SCR reaction [42,50,51]. Recently, Xin et al. [52] designed bifunctional V_a-MnO_x (where *a* represents the molar ratios of V / (V + Mn)) catalysts composed of Mn₂O₃ and Mn₂V₂O₇ phases that significantly improved both NO_x conversion and N₂ selectivity in comparison with Mn₂O₃ at low-temperature (Figure 1). Although Mn₂V₂O₇ showed an excellent N₂ selectivity, the NO_x conversion is much lower on it. Especially, above 90% NO_x conversion and 80% N₂ selectivity was observed in the temperature region of 120–240 °C over the V_{0.05}-MnO_x catalyst. The V_{0.05}-MnO_x catalyst also found to exhibit higher NO_x conversion to N₂ as compared to the mechanically mixed Mn₂O₃ + Mn₂V₂O₇ sample which has the same component content to V_{0.05}-MnO_x (Figure 1). This finding indicated that the synergism between Mn₂O₃ and Mn₂V₂O₇ exists in the chemically prepared V_{0.05}-MnO_x rather than the mechanically mixed Mn₂O₃ + Mn₂V₂O₇ sample. Moreover, the mechanically mixed Mn₂O₃ + Mn₂V₂O₇ sample showed higher activity in comparison to mechanically mixed MoO₃ + Mn₂V₂O₇ sample, suggesting that the presence of Mn₂O₃ phase in the catalyst is necessary for NH₃-SCR reaction. In conjunction with in situ IR characterization and DFT (density functional theory) calculation results, the authors concluded that the Mn₂O₃ phase of the

catalyst could activate NH_3 into NH_2 intermediate, which then transferred to the $\text{Mn}_2\text{V}_2\text{O}_7$ phase of the catalyst and reacted with gaseous NO into NH_2NO . Finally, the generated NH_2NO intermediate on the $\text{Mn}_2\text{V}_2\text{O}_7$ phase exclusively decomposed to the N_2 rather than the undesired byproduct, N_2O , which is formed due to the deep oxidation of adsorbed NH_3 on Mn_2O_3 .

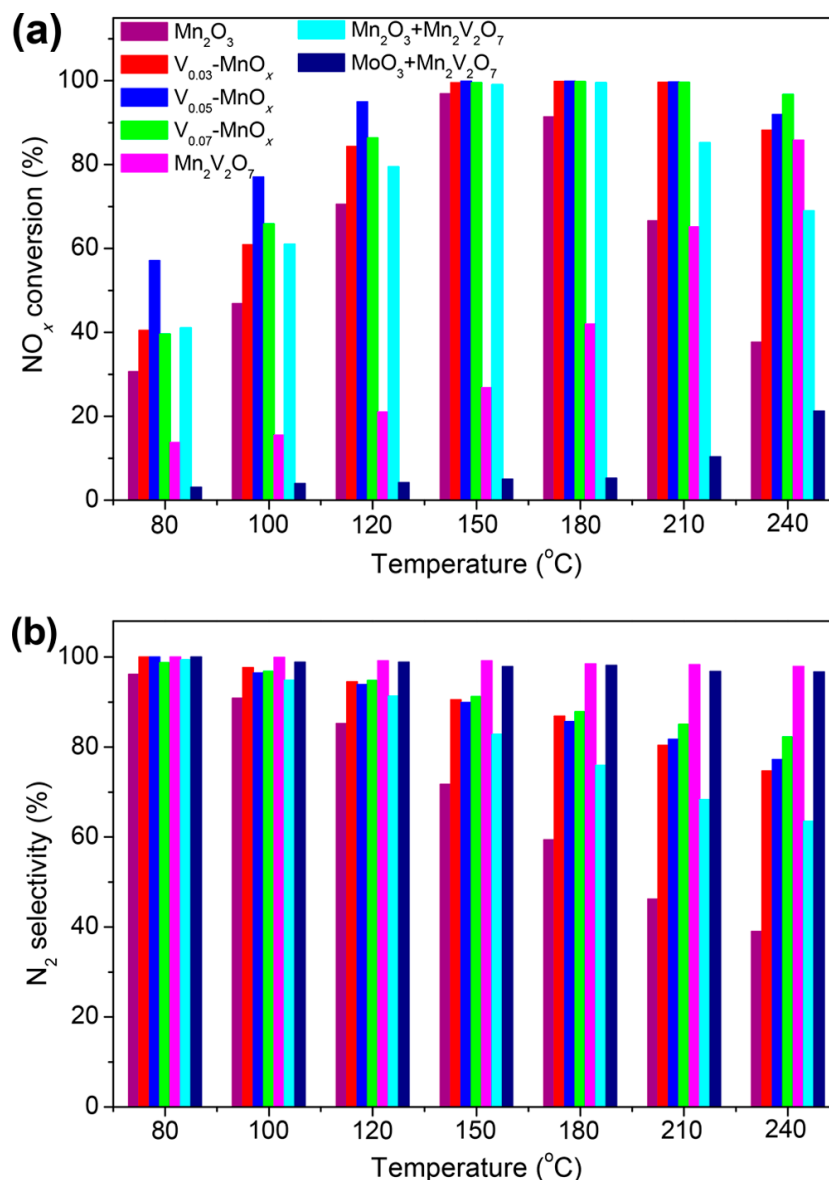


Figure 1. (a) NO_x conversion and (b) N_2 selectivity for $\text{V}_a\text{-MnO}_x$, Mn_2O_3 , $\text{Mn}_2\text{V}_2\text{O}_7$, and reference samples. Reprinted from Reference [52]. Copyright 2018, with Permission from American Chemical Society.

Han and co-workers [53] fabricated triple-shelled NiMn_2O_4 hollow spheres (Figure 2a,b) by using a solvothermal method and tested their ability for low-temperature NH_3 -SCR reaction. As shown in Figure 2c, the prepared NiMn_2O_4 hollow spheres ($\text{NiMn}_2\text{O}_4\text{-S}$) showed the best catalytic activity with NO_x conversion of above 90% over a wide temperature range from 100 °C to 225 °C as compared to the NiMn_2O_4 nanoparticles ($\text{NiMn}_2\text{O}_4\text{-P}$). The triple-layer shell structure of the $\text{NiMn}_2\text{O}_4\text{-S}$ catalyst generates a larger surface area ($165.3 \text{ m}^2 \text{ g}^{-1}$) that exposes more active sites (such as surface Mn^{4+} and surface adsorbed oxygen species), which are responsible for its superior activity. Additionally, the $\text{NiMn}_2\text{O}_4\text{-S}$ catalyst displayed outstanding stability and good tolerance to H_2O and SO_2 (Figure 2d).

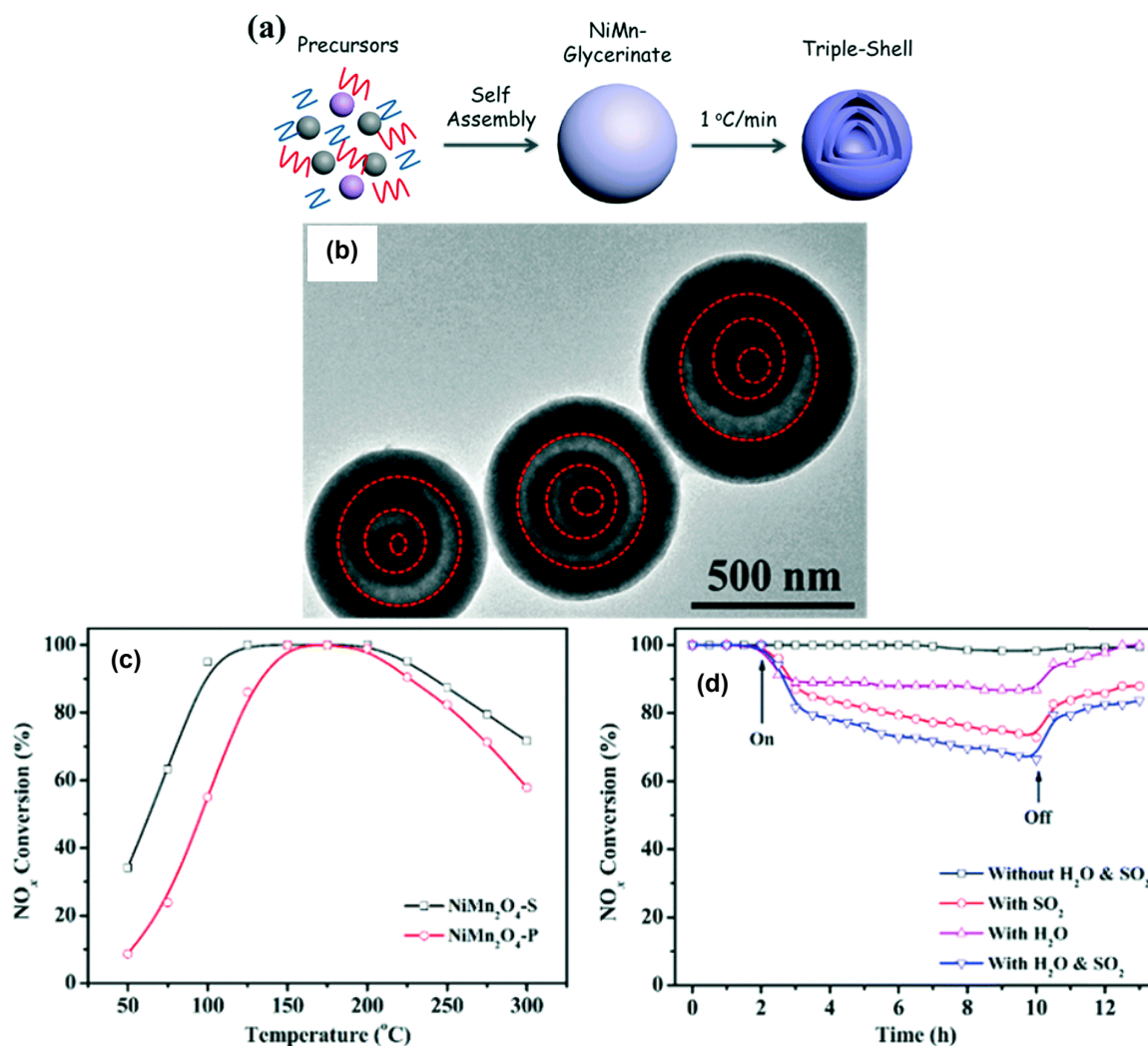


Figure 2. (a) Scheme of the preparation of triple-shelled NiMn₂O₄ hollow spheres and (b) TEM image of NiMn₂O₄-S; (c) NO_x conversion over the NiMn₂O₄ catalysts and (d) durability tests of the NiMn₂O₄-S catalyst at 150 °C. Reaction conditions: [NO] = [NH₃] = 500 ppm, [O₂] = 5 vol%, [SO₂] = 100 ppm (when used), [H₂O] = 5 vol% (when used), balanced with Ar, GHSV = 68,000 h⁻¹. Adapted from Reference [53]. Copyright 2018, with Permission from Royal Society of Chemistry.

Gao et al. [54] investigated the low-temperature NH₃-SCR reaction over the hydroxyl-containing Me-Mn binary oxides (Me = Co, Ni) prepared by a combined complexation-esterification method. It was found that the NO_x conversion decreased in the order of Mn₃O₄-Co₃O₄-OH (Co-MnO_x binary oxide) > Mn₂O₃-NiMnO₃-OH (Ni-MnO_x binary oxide) > Mn₂O₃-OH, while the N₂ selectivity increased in the sequence of Mn₃O₄-Co₃O₄-OH < Mn₂O₃-OH < Mn₂O₃-NiMnO₃-OH. Although the Co and Ni elements in the catalysts delay the poisoning of SO₂ as compared to MnO_x sample, the Co-MnO_x and Ni-MnO_x binary oxides are deactivated by SO₂ over the post-ponement due to the formation of metal sulfate and ammonia hydrogensulfite species. In another study, Sun and co-workers [55] prepared Mn_{0.66}M_{0.33}O_x catalysts (M = Fe, Zn, Cu) and a series of Fe_αMn_{1-α}O_x (α = 1, 0.25, 0.33, 0.50, 0 mol%) catalysts and examined for NH₃-SCR at low-temperatures. The results demonstrated that the Fe_{0.33}Mn_{0.66}O_x catalyst displayed the superior NH₃-SCR activity (NO_x removal efficiency > 90%) in a wide temperature range (75–225 °C) among the Cu_{0.33}Mn_{0.66}O_x, Zn_{0.33}Mn_{0.66}O_x, and Fe_αMn_{1-α}O_x (α = 1, 0.25, 0.50, 0 mol%) catalysts. The authors proposed that the distortion of the catalyst structure by Fe doping could play a key role in improving the NH₃-SCR performance over the Fe_{0.33}Mn_{0.66}O_x catalyst.

Rare-earth metal oxides have been frequently adopted to modify the MnO_x as an efficient low-temperature NH_3 -SCR catalyst due to their incomplete 4f and empty 5d orbitals [50,51,56]. Fan et al. [57] synthesized Gd-modified MnO_x catalysts with Gd/Mn molar ratio of 0.05, 0.1, and 0.3 to improve the catalytic performance and sulfur resistance in the NH_3 -SCR reaction at low-temperature. The MnGdO-2 catalyst (the mole ratio of Gd/Mn = 0.1) found to show the optimal NO conversion and N_2 selectivity among the investigated catalysts. The addition of a proper amount of Gd into MnO_x could enhance the concentrations of surface Mn^{4+} and chemisorbed oxygen species, and increase the amount and the strength of surface acid sites, which lead to better low-temperature catalytic performance than the others. Furthermore, the MnGdO-2 catalyst had an excellent tolerance to $\text{SO}_2/\text{H}_2\text{O}$ as compared to pure MnO_x sample (Figure 3). Their results demonstrate that the doping of Gd could restrains the transformation of MnO_2 to Mn_2O_3 and the generation of MnSO_4 , obstructs the decrease in Lewis acid sites and the increase in Brønsted acid sites, and eases the competitive adsorption between the NO and SO_2 and, thus, improves the resistance to SO_2 .

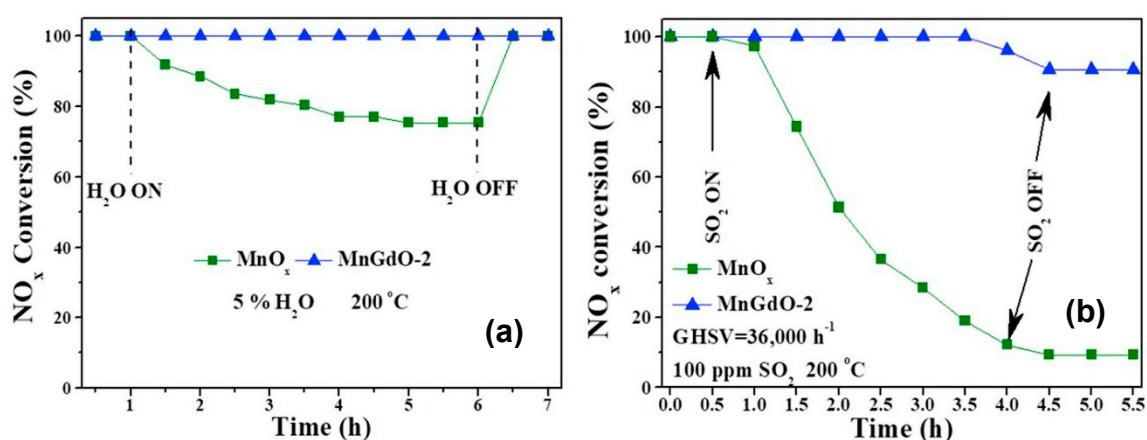


Figure 3. The (a) resistance to water vapor poisoning test and (b) resistance to sulfur poisoning test. (Reaction condition: $[\text{NO}] = [\text{NH}_3] = 500$ ppm, $[\text{O}_2] = 5$ vol%, balanced with N_2 , $[\text{H}_2\text{O}] = 5$ vol%, $[\text{SO}_2] = 100$ ppm, and $\text{GHSV} = 36,000 \text{ h}^{-1}$). Reprinted from Reference [57]. Copyright 2018, with Permission from Elsevier.

Li et al. [58] developed hollow $\text{MnO}_x\text{-CeO}_2$ binary nanotubes as efficient low-temperature NH_3 -SCR catalysts via an interfacial oxidation-reduction process using KMnO_4 aqueous solution and $\text{Ce}(\text{OH})\text{CO}_3$ nanorod as both template and reducing agent without any other intermediate. They reported that the $\text{MnO}_x\text{-CeO}_2$ hollow nanotube catalyst with 3.75 g of $\text{Ce}(\text{OH})\text{CO}_3$ template (denoted it as $\text{MnO}_x\text{-CeO}_2\text{-B}$) exhibited outstanding performance with more than 96% NO_x conversion in the temperature range of 100–180 °C. The best activity of the $\text{MnO}_x\text{-CeO}_2\text{-B}$ catalyst was due to its ample number of surface Mn^{4+} and O species, and hollow and porous structures that provide abundant Lewis acid sites and large surface area. Additionally, $\text{MnO}_x\text{-CeO}_2\text{-B}$ catalyst showed an excellent resistance to H_2O and SO_2 (Figure 4) and especially, the great SO_2 tolerance was ascribed to the hierarchically porous and hollow structure that inhibits the deposition of ammonium sulfate species, and the doping of ceria that acts as an SO_2 trap to limit sulfation of the main active phase.

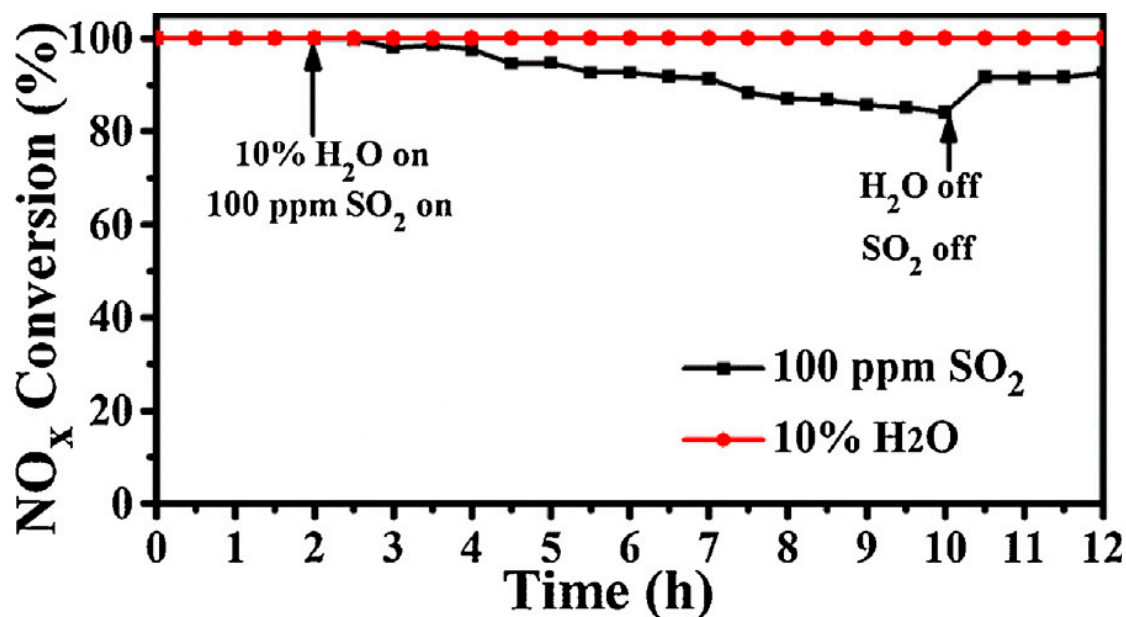
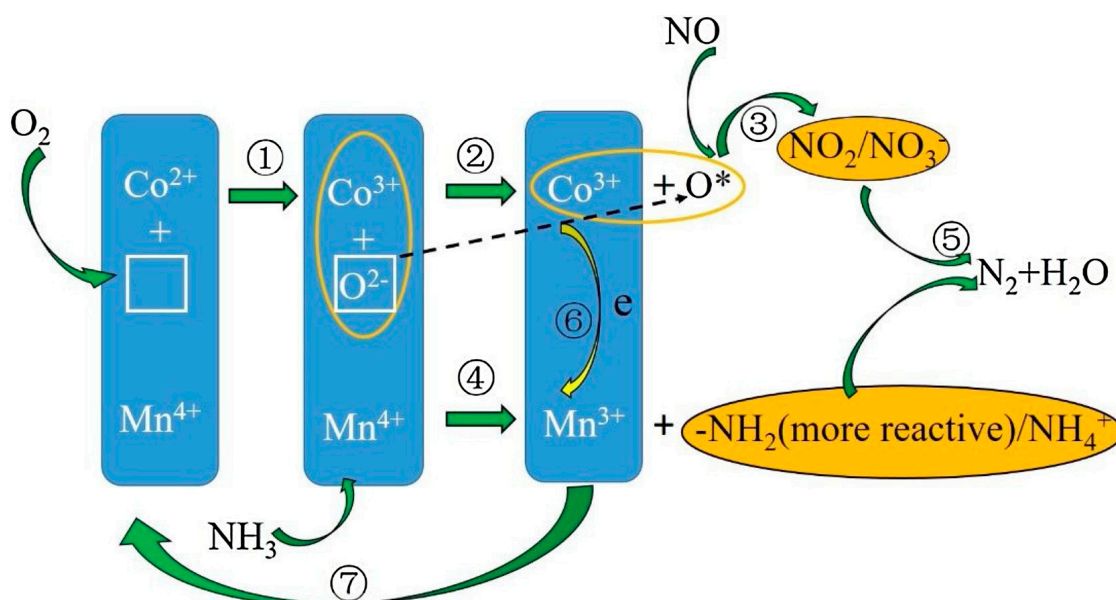


Figure 4. H₂O tolerance and SO₂ tolerance of the MnO_x-CeO₂-B hollow nanotube. Reaction conditions: [NO_x] = [NH₃] = 1000 ppm, [O₂] = 5%, N₂ as balance gas, and GHSV = 30,000 h⁻¹. Reprinted from Reference [58]. Copyright 2018, with Permission from Elsevier.

Fe-based binary catalysts have also been studied as NH₃-SCR catalysts due to their high activity, excellent resistance to H₂O and SO₂, outstanding environmentally friendly performance, lower cost, and higher abundance [59–62]. Mu et al. [63] synthesized a series of vanadium-doped Fe₂O₃ catalysts and evaluated the effect of V on the low-temperature NH₃-SCR activity of hematite. The NH₃-SCR activity and N₂ selectivity are greatly enhanced after the incorporation of vanadium into Fe₂O₃ and the Fe_{0.75}V_{0.25}O₈ catalyst with a Fe/V mole ratio of 3/1 showed the best catalytic performance over a wide temperature window and strong resistance to H₂O and SO₂. They found that the charge transfer from Fe to V due to the electron inductive effect between Fe and V which could enhance the redox ability and surface acidity thereby superior NH₃-SCR activity at low-temperature. The in situ DRIFTS and kinetic studies suggested that the SCR reaction followed the Langmuir–Hinshelwood mechanism below 200 °C, while an Eley–Rideal mechanism dominated at and above 200 °C. Li and co-workers [64] reported novel iron titanium (CT-FeTi) catalyst, prepared by a CTAB-assisted process, showing good deNO_x efficiency and H₂O resistance at low-temperature as compared to the FeTi catalyst that prepared without adding CTAB. The addition of CTAB during the CT-FeTi catalyst preparation not only promotes to form the uniform mesoporous structure to avoid being excessively enlarged in the presence of H₂O, but also enhances the adsorption of bridging nitrate and NH₃ species on Lewis acid sites. Thus, the authors concluded that the CTAB acted as a “structural” and “chemical” promoter in improving the NH₃-SCR activity and H₂O resistance at low-temperature.

Recently, Co-based spinel catalysts have shown to exhibit a remarkable low-temperature NH₃-SCR activity, N₂ selectivity, and tolerance to SO₂/H₂O [30,65–67]. Meng et al. [48] synthesized a highly efficient Co_aMn_bO_x (where a/b is the molar ratio of Co/Mn) mixed oxide catalysts and investigated the effects of the Co/Mn molar ratio on the low-temperature NH₃-SCR reaction. The Co_aMn_bO_x mixed oxides showed higher NH₃-SCR activity than either MnO_x or CoO_x alone due to their improved redox properties and surface acid sites by the synergistic effects between the Co and Mn species. Particularly, the catalyst with Co/Mn molar ratio of 7:3 (Co₇Mn₃O_x) exhibited the greatest activity (>80% NO_x conversion) in a temperature window of 116–285 °C as compared to the catalysts with Co/Mn molar ratio of 5:5 (Co₅Mn₅O_x) and 3:7 (Co₃Mn₇O_x). They considered that the high NO + O₂ adsorption ability and enhanced redox properties of the Co₇Mn₃O_x catalyst, emerging from its MnCo₂O_{4.5} spinel phase and higher surface area, were beneficial to augment the NH₃-SCR performance by forming

nitrate species on the catalyst surface. Although $\text{Co}_7\text{Mn}_3\text{O}_x$ catalyst had better resistance to $\text{H}_2\text{O}/\text{SO}_2$ than the $\text{Co}_3\text{Mn}_7\text{O}_x$ and MnO_x , the tolerance to SO_2 poisoning still need to be improved for practical use. Nevertheless, it was found that the deactivated $\text{Co}_7\text{Mn}_3\text{O}_x$, $\text{Co}_3\text{Mn}_7\text{O}_x$, and MnO_x catalysts in SO_2 stream can be regenerated simply by washing with water. Based on their results, the authors also proposed the NH_3 -SCR reaction mechanism over the $\text{Co}_7\text{Mn}_3\text{O}_x$ catalyst, which is shown in Scheme 1. The reaction was initiated by adsorption and activation of gaseous oxygen on oxygen vacancies (symbol \square), which was then transformed into lattice oxygen O^{2-} (Step 1); This lattice oxygen was diffused to the catalyst surface and then it had become surface active oxygen (O^*) (Step 2); Gaseous NO was adsorbed and subsequently reacted with O^* to form $\text{NO}_2/\text{NO}_3^-$ intermediates (Step 3); Meanwhile, NH_3 was activated to $-\text{NH}_2$ and NH_4^+ species by Mn^{4+} (Step 4); Finally, $\text{NO}_2/\text{NO}_3^-$ intermediates reacted with the NH species to produce reaction products, N_2 , and H_2O (Step 5); By the electron transfer from Mn^{3+} to Co^{3+} (Step 6); the catalyst was recovered to its original state (Step 7); Thus, the synergistic effect between the Co and Mn plays a key role in improving the NH_3 -SCR activity over $\text{Co}_7\text{Mn}_3\text{O}_x$ catalyst.



Scheme 1. The proposed mechanism of the NH_3 -SCR reaction over the $\text{Co}_7\text{Mn}_3\text{O}_x$ catalyst and the synergistic catalytic effect between Mn and Co cations. Reprinted from Reference [48]. Copyright 2018, with Permission from Elsevier.

Mesoporous materials have been proved as promising catalysts for NH_3 -SCR reaction since they can facilitate to promote effective diffusion of reactants towards the active sites [30,65,66,68]. With this perspective, Hu et al. [47] developed mesoporous 3D nanosphere-like Mn-Co-O catalysts through a template-free approach and evaluated for low-temperature NH_3 -SCR reaction. It was found that the synthesized Mn-Co-O samples showed excellent NH_3 -SCR activity in a broad working temperature window of 75 to 325 °C (NO_x conversion above 80%). They ascribed this outstanding performance to the strong and abundant acid sites, the strong adsorption of NO_x , robust redox properties, the formation of more oxygen vacancies and metal-metal interactions between the cobalt and manganese species.

Besides Mn, Fe, and Co oxides, CuO_x has also been considered in the bimetallic catalyst formulations for low-temperature NH_3 -SCR reaction [69,70]. For instance, Ali et al. [71] reported the $\text{Cu}_x\text{-Nb}_{1.1-x}$ ($x = 0.45, 0.35, 0.25, 0.15$) bimetal oxides catalysts and found that the Cu/Nb ratio was crucial in enhancing the NH_3 -SCR activity. As shown in Figure 5a,b, all binary $\text{Cu}_x\text{-Nb}_{1.1-x}$ oxides exhibited significantly higher activity than the CuO_x and Nb_2O_5 , and among the $\text{Cu}_x\text{-Nb}_{1.1-x}$ samples, $\text{Cu}_{0.25}\text{-Nb}_{0.85}$ catalyst displayed the best performance in a wide temperature window of 180–330 °C (>90% NO conversion). Even at a high GHSV of 105,000 h^{-1} , the optimal $\text{Cu}_{0.25}\text{-Nb}_{0.85}$ catalyst

showed a good NO removal efficiency (above 90% NO conversion) from 210 °C to 360 °C (Figure 5c). Although the SO₂/H₂O streams in the feed gas have some adverse impact on Cu_{0.25}-Nb_{0.85}, still the catalyst showed excellent resistance to SO₂/H₂O with reversible deactivation (Figure 5d). The superior NH₃-SCR performance and SO₂/H₂O tolerance of Cu_{0.25}-Nb_{0.85} catalyst were attributed to its high acid amount and NO adsorption capacity.

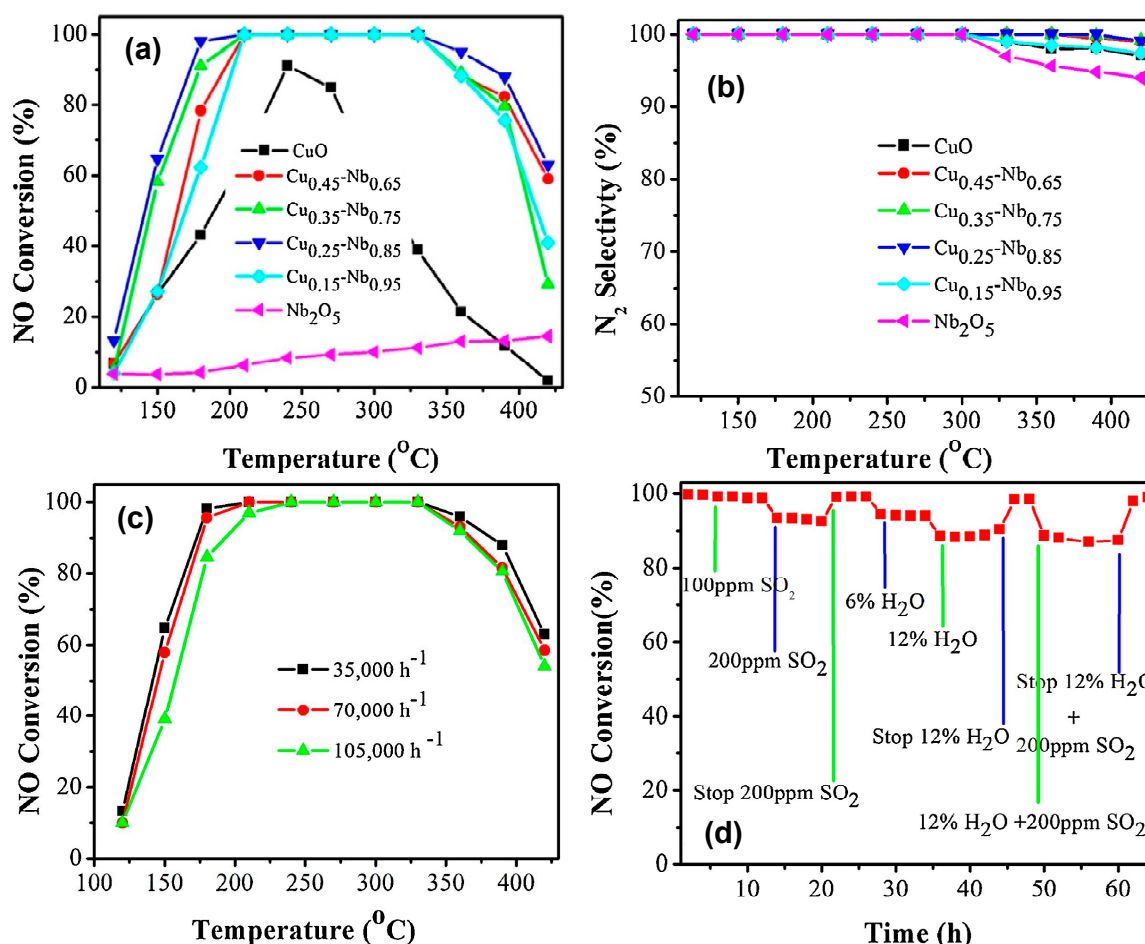


Figure 5. (a) NO conversion; (b) N₂ selectivity over Cu_x-Nb_{1.1-x} (x = 0.45, 0.35, 0.25, 0.15) as a function of temperature under a GHSV of 35,000 h⁻¹; (c) effect of GHSV on NO conversion over Cu_{0.25}-Nb_{0.85}, and (d) effect of SO₂, H₂O, and SO₂ + H₂O on NO conversion over Cu_{0.25}-Nb_{0.85} at 200 °C under a GHSV of 35,000 h⁻¹. (Reaction conditions: [NO] = [NH₃] = 1000 ppm, [O₂] = 3% and N₂ balance), and Effect of SO₂, H₂O, and SO₂ + H₂O on NO conversion over Cu_{0.25}-Nb_{0.85} at 200 °C under a GHSV of 35,000 h⁻¹. Reprinted from Reference [71]. Copyright 2018, with Permission from Elsevier.

3. Ternary and Multi-Transition Metal-Based Catalysts

The catalytic performance of single transition metal oxides can also be improved by mixing with two or multi other metal oxides. Thus, transition metal oxides are widely reported to fabricate ternary- or multi-metal-based low-temperature NH₃-SCR catalysts, which could improve the catalytic activity by the enlarged synergetic interactions [14,72–87]. Fang et al. [88] investigated the low-temperature NH₃-SCR reaction over the Fe_{0.3}Mn_{0.5}Zr_{0.2} catalyst and found that it showed an excellent deNO_x activity with 100% NO conversion in the temperature range of 200–360 °C as compared to the Fe_{0.5}Zr_{0.5} and Mn_{0.5}Zr_{0.5} samples. Moreover, the Fe_{0.3}Mn_{0.5}Zr_{0.2} catalyst had outstanding stability and good tolerance to SO₂ (Figure 6), which they attributed to the strong interactions among Fe, Mn, and Zr species. However, the durability of the catalyst in the presence of both SO₂ and H₂O need to be tested to investigate its feasibility in practical use.

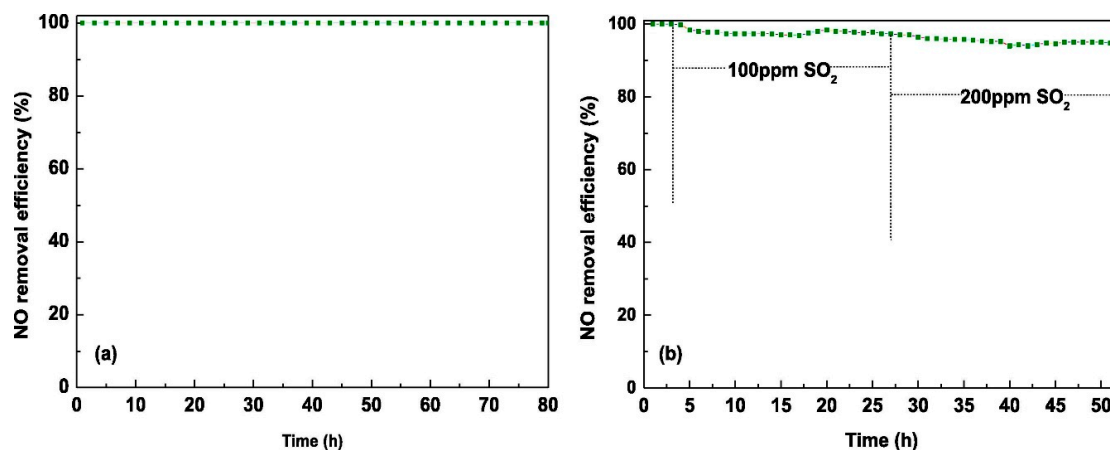


Figure 6. (a) NO removal efficiency of $\text{Fe}_{0.3}\text{Mn}_{0.5}\text{Zr}_{0.2}$ as a function of time at 200 °C and (b) effect of SO_2 on the NO removal over $\text{Fe}_{0.3}\text{Mn}_{0.5}\text{Zr}_{0.2}$ at 200 °C. Reprinted from Reference [88]. Copyright 2017, with Permission from Elsevier.

Guo and co-workers [89] studied the effect of Sb doping on the activity of MnTiO_x catalyst for NH_3 -SCR reaction. The results showed that Sb modification has greatly improved the NH_3 -SCR performance of MnSbTiO_x catalysts in comparison to the MnTiO_x and SbTiO_x samples. Particularly, the $\text{MnSbTiO}_x\text{-0.2}$ (Sb/Mn molar ratio = 0.2) catalyst exhibited the best activity with above 90% NO_x conversion in the temperature range of 138–367 °C as it had good adsorption and activation properties for NH_3 and NO_x reactants in SCR. It can be seen from Figure 7 that the addition of Sb dramatically improved the SO_2 and H_2O resistance of MnTiO_x catalyst. Although the NO_x conversion over the $\text{MnSbTiO}_x\text{-0.2}$ catalyst slightly decreased in the presence of SO_2 and H_2O , it recovered to almost the original level after stopping the $\text{SO}_2/\text{H}_2\text{O}$ supply.

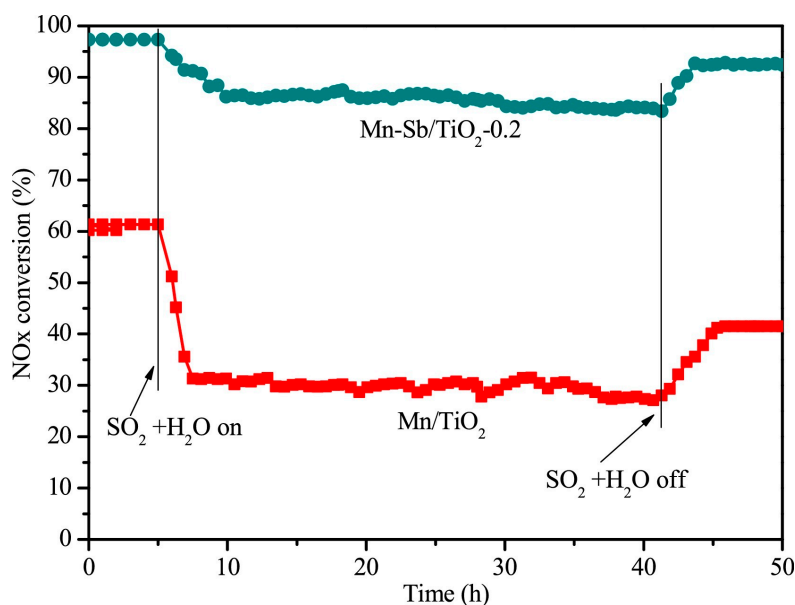


Figure 7. SO_2 resistance of MnTiO_x and $\text{MnSbTiO}_x\text{-0.2}$ catalysts at 150 °C. Reaction conditions: 600 ppm NO , 600 ppm NH_3 , 5% O_2 , 5% H_2O , 100 ppm SO_2 , balance Ar, $\text{GHSV} = 108,000 \text{ h}^{-1}$. Reprinted from Reference [89]. Copyright 2018, with Permission from Elsevier.

Shi et al. [90] synthesized a series of $\text{Ni}_y\text{Co}_{1-y}\text{Mn}_2\text{O}_x$ microspheres (MSs) ($y = 0.1, 0.3, 0.5, 0.7, 0.9$) for NH_3 -SCR using a hydrothermal method. It was observed that the activity of all ternary MSs was greater than binary CoMn_2O_x and NiMn_2O_x , and $\text{Ni}_{0.7}\text{Co}_{0.3}\text{Mn}_2\text{O}_x$ showed the best NH_3 -SCR performance among the $\text{Ni}_y\text{Co}_{1-y}\text{Mn}_2\text{O}_x$ catalysts. Although the $\text{Ni}_{0.7}\text{Co}_{0.3}\text{Mn}_2\text{O}_x$ catalyst exhibited

good resistance to H₂O, it had poor SO₂ tolerance which needs to be improved. Wu and co-workers [91] compared the DeNO_x performance of MnO₂/CoAl-LDO and CoMnAl-LDO mixed metal oxides prepared from CoAl-MnO₂-LDH and CoMnAl-LDH templates by ion-exchange/redox reaction and hexamethylenetetramine (HMT) hydrolysis methods, respectively. The CoAl-MnO₂-LDH showed higher NH₃-SCR activity in a broad temperature window of 90–300 °C (Figure 8a) as well as better stability and SO₂/H₂O resistance (Figure 8b) than the CoMnAl-LDO, which was attributed to its larger specific surface area, stronger redox ability, more quantitative acid sites, and abundant active components.

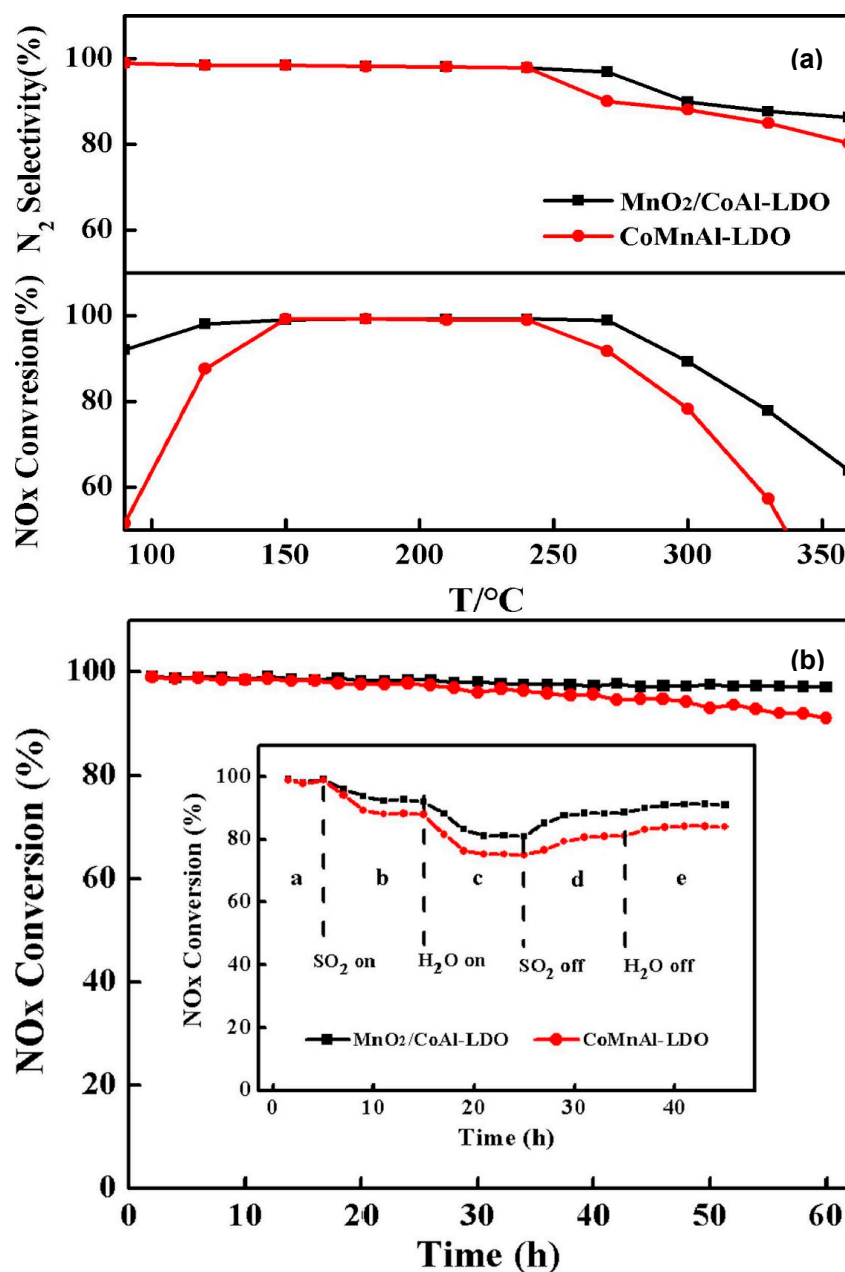


Figure 8. (a) NO_x conversion and N₂ selectivity over MnO₂/CoAl-LDO and CoMnAl-LDO catalysts prepared by calcination at 500 °C; and (b) the stability and SO₂/H₂O resistance test (inset) of MnO₂/CoAl-LDO and CoMnAl-LDO catalysts at 240 °C. Reaction conditions: [NH₃] = 600 ppm, [NO] = 600 ppm, [O₂] = 5 vol%, 100 ppm SO₂ (when used), 10 vol% H₂O. (when used) balanced by N₂. Reprinted from Reference [91]. Copyright 2019, with Permission from Elsevier.

Leng and collaborators [92] synthesized $\text{Mn}_{0.2}\text{TiO}_x$, $\text{Ce}_{0.3}\text{TiO}_x$ and series of $\text{Mn}_a\text{Ce}_{0.3}\text{TiO}_x$ ($a = 0.1, 0.2, 0.3$) catalysts and investigated their applicability for low-temperature NH_3 -SCR reaction. They demonstrated that the low-temperature NH_3 -SCR activity of $\text{Mn}_a\text{Ce}_{0.3}\text{TiO}_x$ was greatly improved after incorporation of Mn, and the $\text{Mn}_{0.1}\text{Ce}_{0.3}\text{TiO}_x$ catalyst displayed the best performance (with 100% NO conversion and above 90% N_2 selectivity) in the temperature range of 175–400 °C even at high GHSV of 80,000 h^{-1} . The outstanding performance of $\text{Mn}_{0.1}\text{Ce}_{0.3}\text{TiO}_x$ catalyst in NH_3 -SCR resulted from its enhanced acidity and chemisorbed oxygen, and suitable redox property derived from $\text{Ce}^{3+} + \text{Mn}^{4+} \leftrightarrow \text{Ce}^{4+} + \text{Mn}^{3+}$ reaction. Furthermore, the NO conversion over the $\text{Mn}_{0.1}\text{Ce}_{0.3}\text{TiO}_x$ decreased and stabilized at 82% after the introduction of 100 ppm SO_2 and 6% H_2O and restored to almost 100% NO conversion after stopping the supply of SO_2 and H_2O (Figure 9), suggesting that the catalyst had excellent resistance to $\text{SO}_2/\text{H}_2\text{O}$ and the effects were reversible.

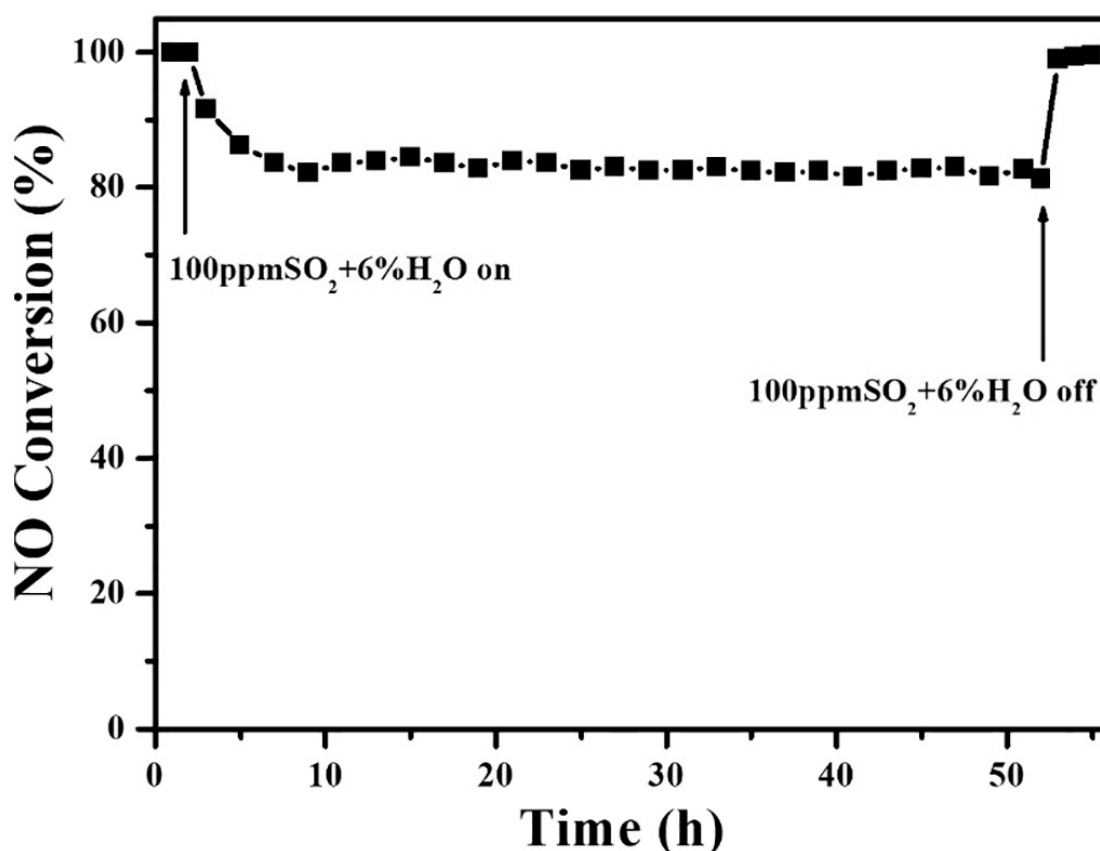


Figure 9. Effect of H_2O and SO_2 on NO conversion over the $\text{Mn}_{0.1}\text{Ce}_{0.3}\text{TiO}_x$ catalyst at 200 °C (1000 ppm NO, 1000 ppm NH_3 , 3% O_2 , balance N_2 , GHSV = 40,000 h^{-1}). Reprinted from Reference [92]. Copyright 2018, with Permission from Elsevier.

Ali et al. [93] developed a series of Nb-promoted $\text{Fe}_x\text{-Nb}_{0.5-x}\text{-Ce}_{0.5}$ ($x = 0.45, 0.4, 0.35$) oxides for NH_3 -SCR. The best activity (>90% NO conversion and near 100% N_2 selectivity) in the broad temperature window of 180–400 °C as well as excellent $\text{SO}_2/\text{H}_2\text{O}$ resistance (Figure 10) was observed for $\text{Fe}_{0.4}\text{-Nb}_{0.1}\text{-Ce}_{0.5}$ catalyst. The authors considered the strong interaction among Nb, Fe, and Ce oxides leading to the enhancement of BET surface area, redox ability, acid amount, and NO adsorption capacity, which could be responsible for the outstanding performance of the catalyst.

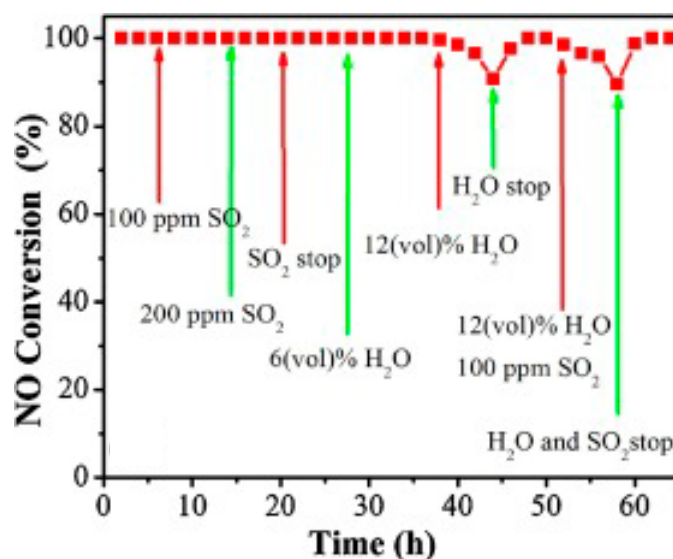


Figure 10. Effect of SO_2 , H_2O , and $\text{SO}_2 + \text{H}_2\text{O}$ on NO conversion over the $\text{Fe}_{0.4}\text{-Nb}_{0.1}\text{-Ce}_{0.5}$ catalyst at $220\text{ }^\circ\text{C}$. Reprinted from Reference [93]. Copyright 2018, with Permission from Elsevier.

Sun and co-workers [94] reported the multimetallic Sm- and/or Zr-doped $\text{MnO}_x\text{-TiO}_2$ catalysts for $\text{NH}_3\text{-SCR}$ reaction. As shown in Figure 11, the Sm and Zr co-doped $\text{MnO}_x\text{-TiO}_2$ (MSZTO_x) catalyst had better activity ($\approx 100\%$ NO conversion and $>95\%$ N_2 selectivity) in a wide temperature range ($125\text{--}275\text{ }^\circ\text{C}$) with an excellent $\text{H}_2\text{O}/\text{SO}_2$ tolerance than the MSTO_x ($\text{MnO}_x\text{-SmO}_x\text{-TiO}_2$), MZTO_x ($\text{MnO}_x\text{-ZrO}_x\text{-TiO}_2$) and MTO_x ($\text{MnO}_x\text{-TiO}_2$) catalysts. The authors claimed that the enhanced redox properties and acidic sites play a crucial role in improving the $\text{NH}_3\text{-SCR}$ performance of MSZTO_x catalyst. Yan and co-workers [95] fabricated $\text{Cu}_{0.5}\text{Mg}_{1.5}\text{Mn}_{0.5}\text{Al}_{0.5}\text{O}_x$ catalyst from layered double hydroxides and found that it showed better activity in a wide temperature range together with superior SO_2 and H_2O tolerance than conventional $\text{Mn}/\gamma\text{-Al}_2\text{O}_3$. The improved performance of $\text{Cu}_{0.5}\text{Mg}_{1.5}\text{Mn}_{0.5}\text{Al}_{0.5}\text{O}_x$ was attributed to the high specific surface area, high reducibility of MnO_2 and CuO species, an abundance of acid sites, and the good dispersion of MnO_2 and CuO species.

Chen et al. [96] investigated the $\text{NH}_3\text{-SCR}$ reaction over a series of $\text{Co}_{0.2}\text{Ce}_x\text{Mn}_{0.8-x}\text{Ti}_{10}$ ($x = 0, 0.05, 0.15, 0.25, 0.35,$ and 0.40) oxides catalysts and observed that the $\text{Co}_{0.2}\text{Ce}_{0.35}\text{Mn}_{0.45}\text{Ti}_{10}$ catalyst exhibited the best catalytic performance with 100% NO conversion and over 91% N_2 selectivity in a broad temperature window of $180\text{--}390\text{ }^\circ\text{C}$. Although NO_x conversion decreased to some extent after introducing SO_2 and H_2O , the $\text{Co}_{0.2}\text{Ce}_{0.35}\text{Mn}_{0.45}\text{Ti}_{10}$ catalyst showed excellent resistance to $\text{SO}_2/\text{H}_2\text{O}$ with reversible inhibition effect (Figure 12). It was concluded that the interactions among Ce, Co, Mn, and Ti oxides led to more surface Brønsted acid and Lewis acid sites, NO_x adsorption sites and modest redox ability which could play a crucial role to improve the $\text{NH}_3\text{-SCR}$ activity of $\text{Co}_{0.2}\text{Ce}_{0.35}\text{Mn}_{0.45}\text{Ti}_{10}$.

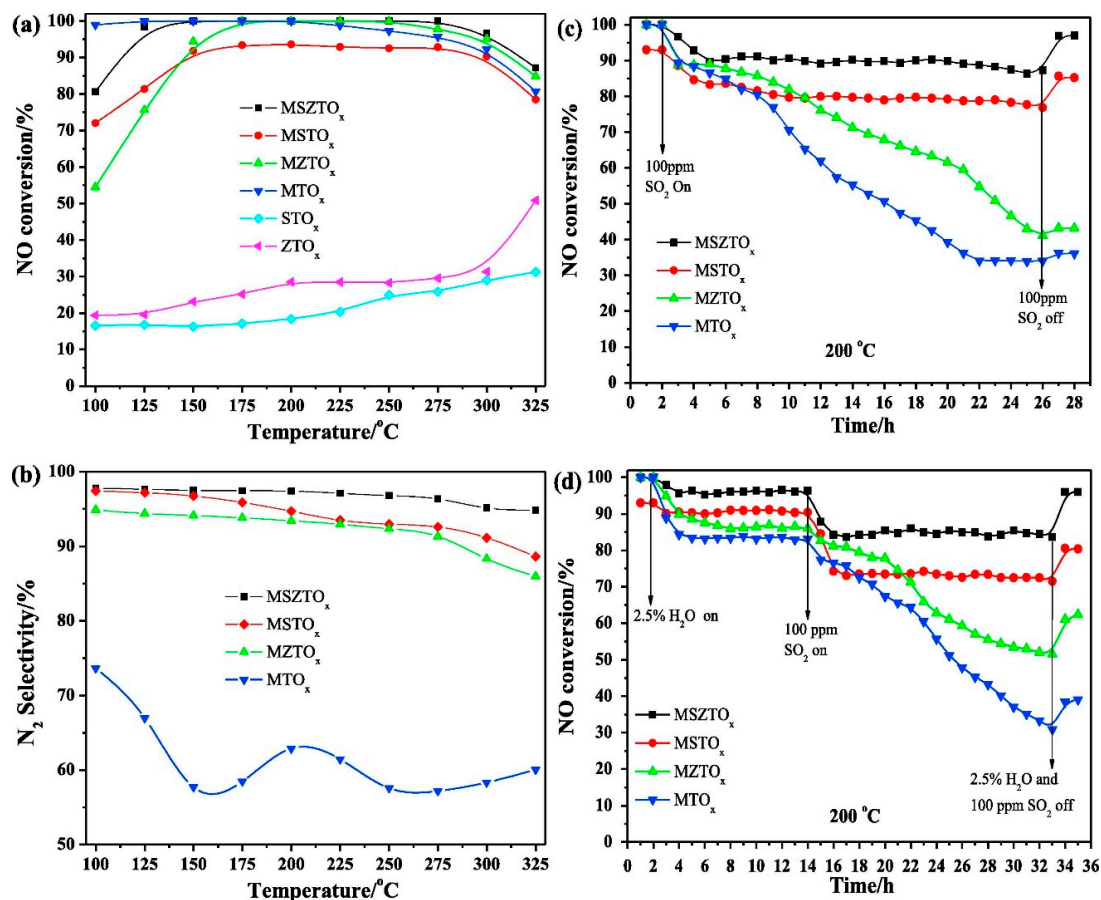


Figure 11. (a) NO conversions and (b) N₂ selectivities of the catalysts in the NH₃-SCR reaction as a function of temperature; (c) SO₂ (100 ppm) resistance tests, and (d) H₂O + SO₂ (2.5 vol%, 100 ppm) resistance tests at 200 °C over the catalysts. Reproduced from Reference [94]. Copyright 2018, with Permission from Elsevier.

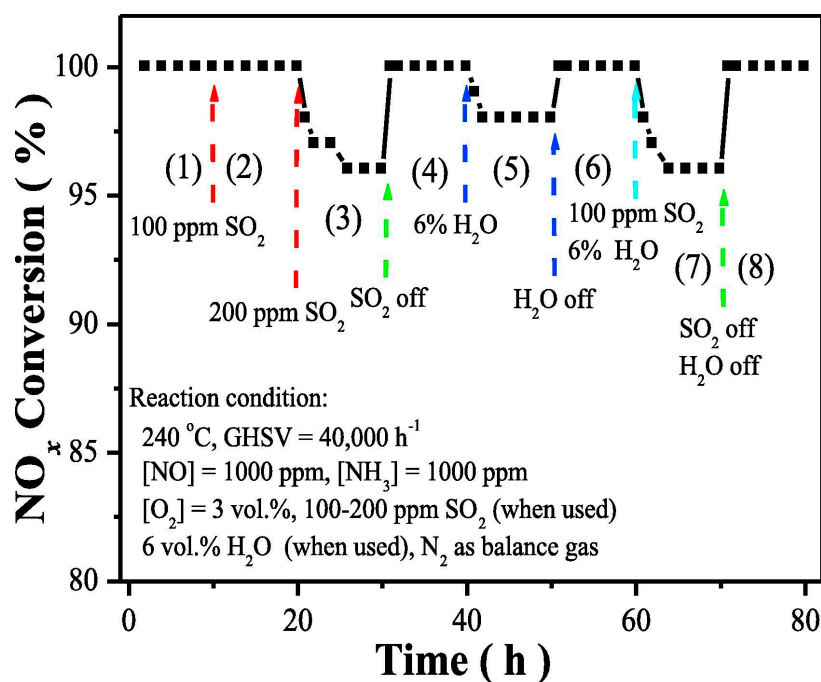


Figure 12. Effects of H₂O and/or SO₂ on NO_x conversion over the Co_{0.2}Ce_{0.35}Mn_{0.45}Ti₁₀ catalyst. Reproduced from Reference [96]. Copyright 2018, with Permission from Elsevier.

4. Supported Single Transition Metal-Based Catalysts

Support materials have proved to be highly beneficial for enhancing the activity and durability of catalysts as they possess high surface area and good thermal stability. In virtue of the fine dispersion of the active component on the surface of the support and the synergistic effect between active component and support, supported catalysts exhibit improved NH_3 -SCR performance than the unsupported transition metal oxide. Therefore, a lot of attention has been focused to increase the de- NO_x efficiency by dispersing the transition metal oxides over different support materials such as TiO_2 , Al_2O_3 , SiO_2 , carbon nanotubes (CNTs), etc. TiO_2 supported transition metal oxides, especially manganese oxides, have been widely reported as promising catalysts for NH_3 -SCR reaction at low temperature [17,24,97–105]. Smirniotis and co-workers [17,106,107] first reported the transition metal oxides (V, Cr, Mn, Fe, Co, Ni, and Cu) supported on Hombikat TiO_2 for NH_3 -SCR reaction at low-temperature. Among the investigated samples, the Mn/Hombikat TiO_2 catalyst found to exhibit the highest activity even in the presence of water. They also studied the effect of different supports on the NH_3 -SCR performance and observed that the Mn/Hombikat TiO_2 (anatase, high surface area) had the best activity as compared to the Kemira TiO_2 (rutile), Degussa P25 TiO_2 (anatase, rutile), Aldrich TiO_2 (anatase, low surface area), Puralox $\gamma\text{-Al}_2\text{O}_3$, Aldrich SiO_2 supported Mn catalysts. It was concluded that the Lewis acidity, redox behavior, and a high surface concentration of MnO_2 could play a key role in improving the NH_3 -SCR activity. Later, they investigated the effect of Mn loading on the NH_3 -SCR performance of Mn/Hombikat TiO_2 and reported that the catalyst with 16.7 wt% Mn had optimal activity and excellent tolerance to H_2O during 10 days of the reaction [108]. In another work, they also proposed the NH_3 -SCR reaction mechanism over the Mn/ TiO_2 catalyst using transient isotopic labeled and in-situ FT-IR studies. As shown in Figure 13, the reaction proceeds via a Mars-van-Krevelen-like mechanism, in which NH_3 and NO species were first adsorbed onto the Mn^{4+} sites (Lewis acid sites), followed by the formation of nitrosamide and azoxy intermediate species. Finally, these intermediates converted into N_2 and H_2O products [24].

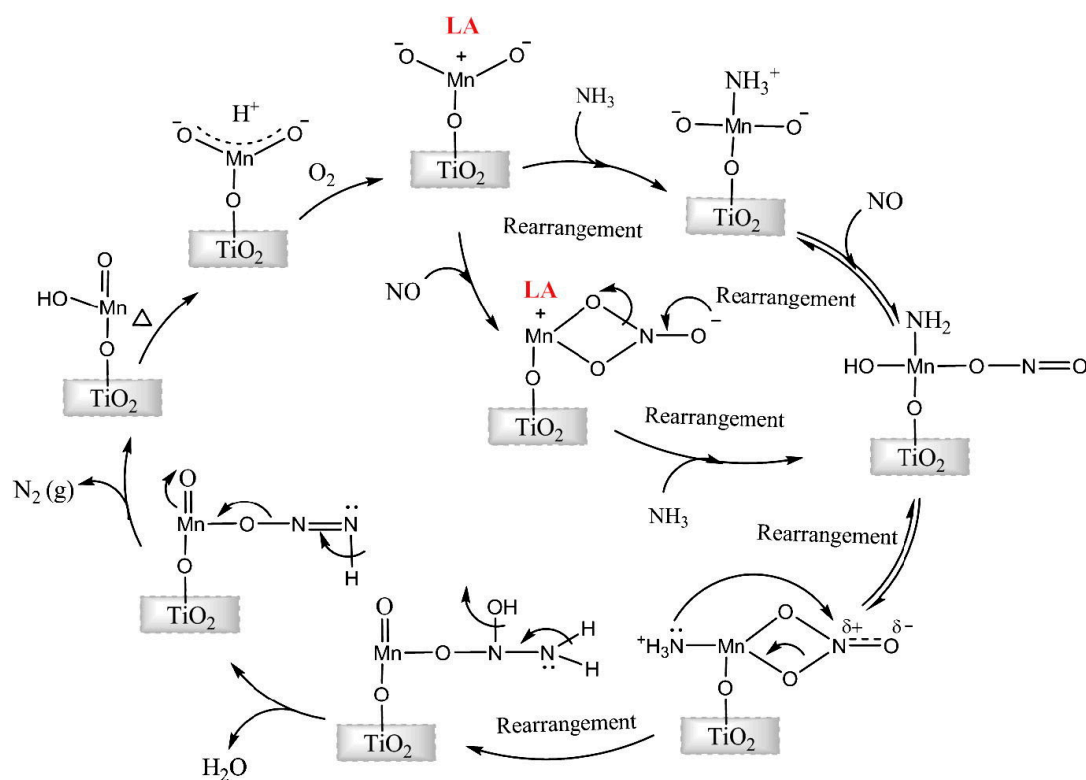


Figure 13. Plausible SCR mechanism over the surface of Mn/ TiO_2 catalyst. Adapted from Reference [24]. Copyright 2012, with Permission from Elsevier.

In the aspect of catalyst structure design, Smirniotis and co-workers [26] developed a series of manganese confined titania nanotube (Mn/TNT-X) catalysts using different TiO₂ precursors (X = Ishihara (I), Kemira (K), Degussa P25 (P25), Sigma–Aldrich (SA), Hombikat (H), TiO₂ synthesized from titanium oxysulfate (TOS)) for low-temperature NH₃-SCR reaction. As can be observed from the Figure 14, all Mn/TNT-X catalysts exhibited an excellent NO_x conversion in broad temperature window, and especially, Mn(0.25)/TNT-H sample obtained the superior activity in the temperature range of 100–300 °C as compared to other catalysts. They believed that the better performance of Mn(0.25)/TNT-H catalyst was due to the high surface area (421 m²/g) of the TNT-H support, and high dispersion of active components. The Mn(0.25)/TNT-H catalyst also showed greater catalytic performance than the conventional Mn-loaded titania nanoparticles (Mn/TiO₂), suggesting that the unique multiwall nanotube with open-ended structure could be advantageous to promote the reaction. Besides, the Mn (0.25)/TNT-H displayed outstanding tolerance to 10 vol% H₂O in the feed (Figure 15), which might be attributed to the preferential existence of highly active and redox potential pairs of Mn⁴⁺ and Mn³⁺ in the tubular framework.

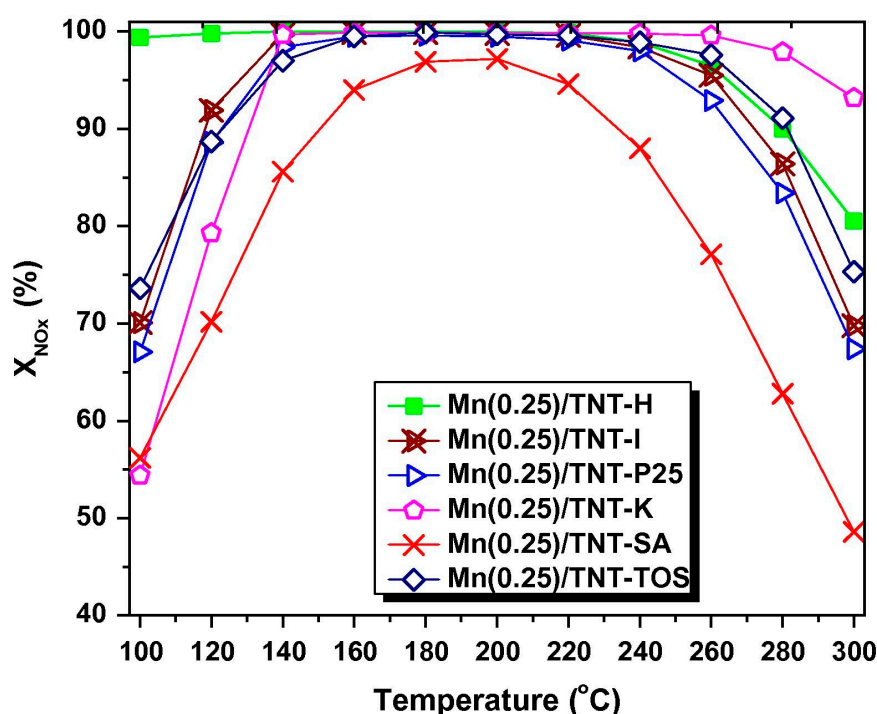


Figure 14. Catalytic evaluation of the Mn(0.25)/TNT-X (X = Hombikat, Ishihara, P25 Degussa, Kemira, Sigma–Aldrich, and Titania oxysulfate) family of catalyst for the SCR of NO_x by NH₃, in the presence of 900 ppm NO, 100 ppm NO₂, 1000 ppm NH₃, 10 vol% O₂ with He balance under a GHSV of 50,000 h⁻¹ in the temperature range from 100–300 °C. Reproduced from Reference [26]. Copyright 2016, with Permission from Elsevier.

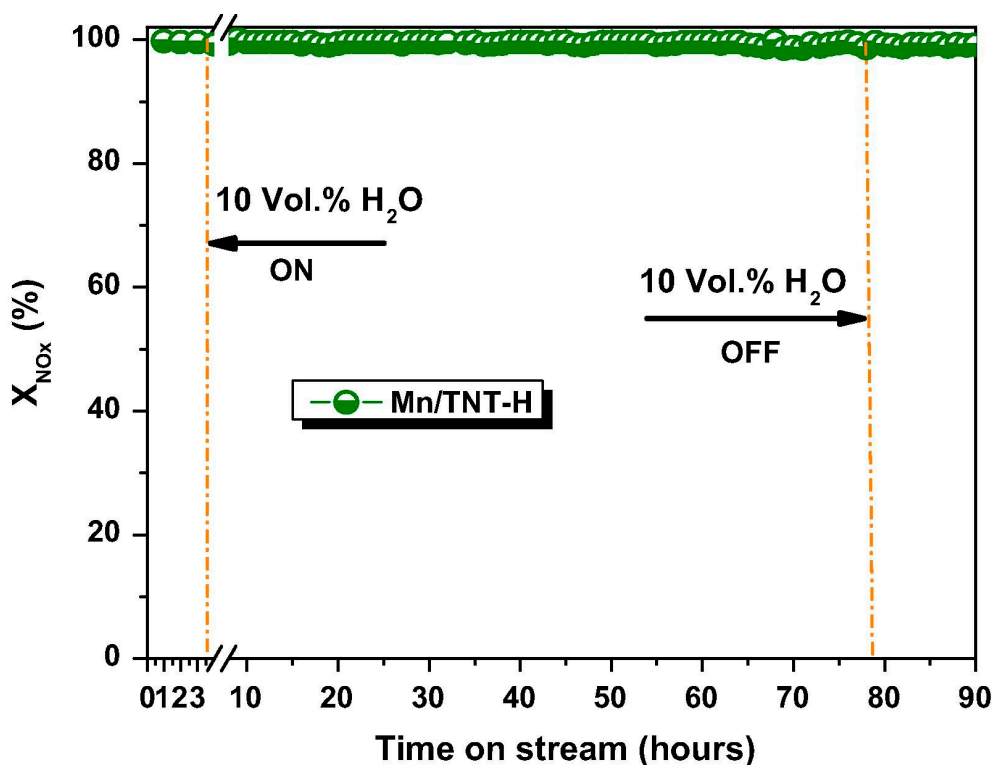


Figure 15. Influence of inlet water concentrations (10 vol%) on NO_x conversion in the SCR reaction over $\text{Mn}(0.25)/\text{TNT-H}$ catalyst at $140\text{ }^\circ\text{C}$; feed: $\text{NO} = 900\text{ ppm}$, $\text{NO}_2 = 100\text{ ppm}$, NH_3/NO_x (ANR) = 1.0, $\text{O}_2 = 10\text{ vol}\%$, He carrier gas, GHSV = $50,000\text{ h}^{-1}$. Reproduced from Reference [26]. Copyright 2016, with Permission from Elsevier.

Recently, Boningari et al. [109] extended this work by comparing the NH_3 -SCR activity of various metal oxide confined titania nanotubes M/TNT ($\text{M} = \text{Mn}, \text{Cu}, \text{Ce}, \text{Fe}, \text{V}, \text{Cr},$ and Co) based on the Hombikat TiO_2 support. As shown in Figure 16, the Mn-, V-, Cr-, and Cu-oxide confined titania nanotubes had excellent low-temperature activity and meanwhile, vanadium oxide confined titania nanotubes showed a broad operation temperature window for the NH_3 -SCR reaction.

Sheng et al. [100] synthesized core-shell $\text{MnO}_x/\text{TiO}_2$ nanorod catalyst, showed high activity, stability, and N_2 selectivity in NH_3 -SCR. They concluded that the abundant mesopores, Lewis-acid sites, and high redox capability could be beneficial to improve catalytic performance. Although the $\text{MnO}_x/\text{TiO}_2$ catalyst exhibited excellent resistance to H_2O , it was deactivated in the presence of SO_2 and $\text{SO}_2/\text{H}_2\text{O}$. Jia et al. [110] reported the low-temperature NH_3 -SCR efficiency of $\text{MnO}_x/\text{TiO}_2$, $\text{MnO}_x/\text{ZrO}_2$, and $\text{MnO}_x/\text{ZrO}_2\text{-TiO}_2$ catalysts, and found that $\text{MnO}_x/\text{ZrO}_2\text{-TiO}_2$ obtained good activity at a temperature of $80\text{--}360\text{ }^\circ\text{C}$ and excellent resistance to H_2O at $200\text{ }^\circ\text{C}$. However, all the catalysts showed poor tolerance to SO_2 and $\text{SO}_2/\text{H}_2\text{O}$ that caused irreversible deactivation. Similar findings were also observed by Zhang et al. [111] over the Mn/Ti, Mn/Zr, and Mn/Ti-Zr catalysts, in which Mn/Ti-Zr sample exhibited an excellent NH_3 -SCR performance in a wide temperature range due to its high surface area, Lewis acid sites, and surface Mn^{4+} ions.

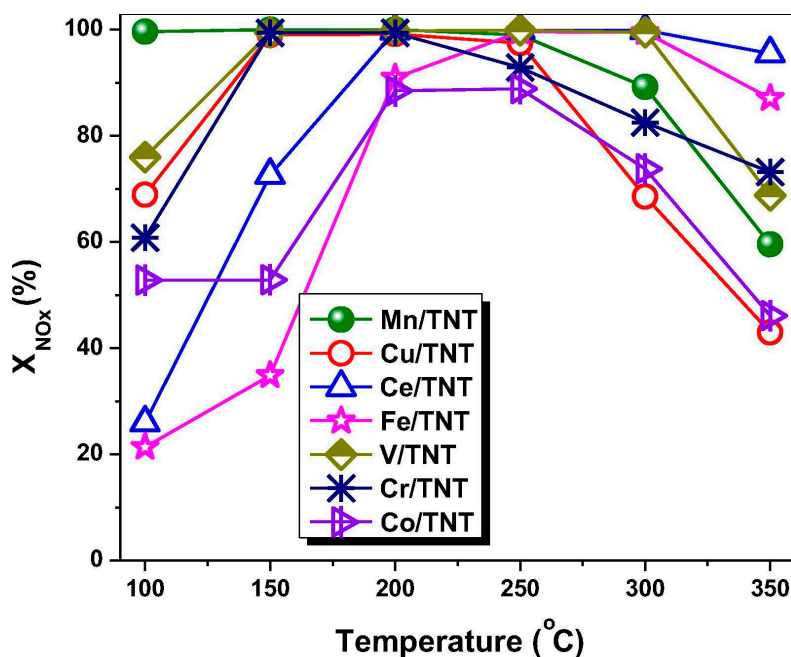


Figure 16. Catalytic activity evaluation of metal oxides confined titania (made of Hombikat titania) nanotube catalytic formulations M/TNT where M = Mn, Cu, Ce, Fe, V, Cr, and Co for the selective catalytic reduction of NO_x by NH₃ in the presence of 900 ppm NO, 100 ppm NO₂, 1000 ppm NH₃, 10 vol% O₂ in He balance, under a GHSV = 50,000 h⁻¹. Reprinted from Reference [109]. Copyright 2018, with Permission from Elsevier.

Carbon nanotubes (CNTs) have been reported as promising catalyst support for NH₃-SCR catalysis due to their excellent stability and unique electronic and structural properties [36,112–115]. Qu and co-workers [116] reported that the NH₃-SCR performance of Fe₂O₃ was dramatically enhanced when it supported on CNTs (Figure 17a). It was concluded that the large surface area, fine dispersion of Fe₂O₃, and interaction between Fe₂O₃ and CNTs were important factors to improve the NH₃-SCR activity. In addition, the Fe₂O₃/CNTs catalyst showed an excellent tolerance to H₂O/SO₂. Interestingly, SO₂ stream in the feed had promoting effect on the NO conversion (Figure 17b), which could be attributed to the increased acid sites for NH₃ adsorption and activation on the catalyst surface in presence of SO₂. Bai et al. [117] developed CNTs supported copper oxide catalysts, and found that the 10 wt% CuO/CNTs showed good NH₃-SCR activity and excellent stability at 200 °C. The 10 wt% CuO/CNTs also had greater performance in comparison to 10 wt% CuO/TiO₂. However, it exhibited poor resistance to SO₂ and moderate tolerance to H₂O.

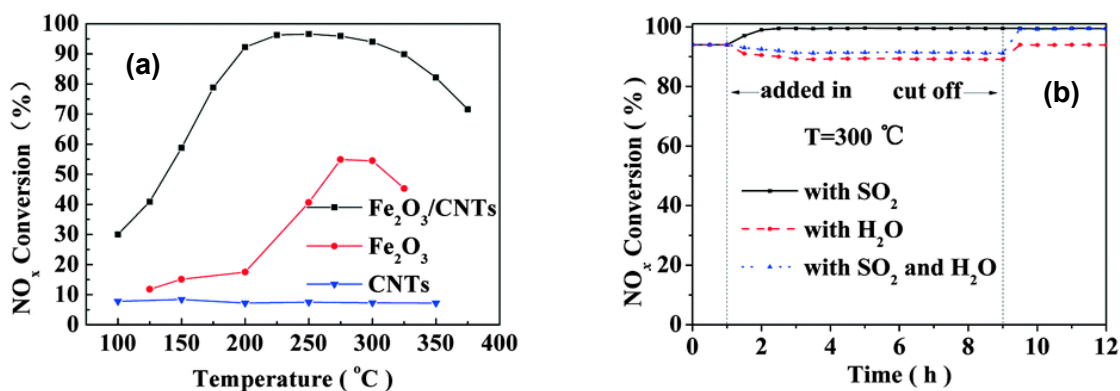


Figure 17. (a) NO_x conversion as a function of temperature over different catalysts and (b) SO₂/H₂O tolerance of the Fe₂O₃/CNTs catalyst. Reprinted from Reference [116]. Copyright 2015, with Permission from Royal Society of Chemistry.

5. Supported Binary and Multi Transition Metal-Based Catalysts

Given that the dispersion of two active components on support enhances the active sites further, researchers have been widely reported the supported binary transition metal-based oxides to improve the performance and $\text{SO}_2/\text{H}_2\text{O}$ tolerance in $\text{NH}_3\text{-SCR}$ reaction. With this perspective, several composites, such as MnCe/CNTs [118], $\text{Mn-Fe}/\text{TiO}_2$ [119], $\text{MnO}_x\text{-CeO}_2/\text{graphene}$ [120], $\text{Mg-MnO}_x/\text{TiO}_2$ [121], $\text{CeO}_x\text{-MnO}_x/\text{TiO}_2\text{-graphene}$ [122], $\text{Fe-Mn}/\text{Al}_2\text{O}_3$ [123], $\text{Mn-Fe}/\text{W-Ti}$ [124], $\text{MnO}_x\text{-CeO}_2/\text{TiO}_2\text{-1\%NG}$ (NG = N-doped grapheme) [125], $\text{Mn-Ce}/\text{CeAPSO-34}$ [126], etc., were investigated for the $\text{NH}_3\text{-SCR}$ reaction at low-temperature. Smirniotis et al. [22] studied the promotional effect of co-doped metals (Cr, Fe, Co, Ni, Cu, Zn, Ce, and Zr) on the $\text{NH}_3\text{-SCR}$ performance of Mn/TiO_2 . As shown in Figure 18, except Zn and Zr, all other co-doped metals had a positive impact on the activity of Mn/TiO_2 , and particularly, the $\text{Mn-Ni}/\text{TiO}_2$ exhibited the highest NO conversion and N_2 selectivity among the other titania-supported bimetallic catalysts.

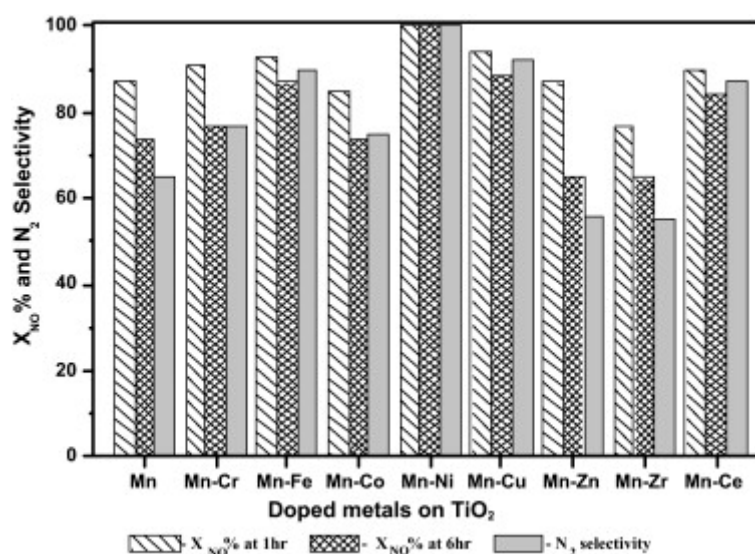


Figure 18. N_2 selectivity and catalytic performance of $\text{Mn-M}'/\text{TiO}_2$ anatase ($\text{M}' = \text{Cr, Fe, Co, Ni, Cu, Zn, Zr, and Ce}$) catalysts: $\text{NH}_3 = 400$ ppm; $\text{NO} = 400$ ppm; $\text{O}_2 = 2.0$ vol%; $\text{GHSV} = 50,000$ h^{-1} ; catalyst wt. = 0.1 g; reaction temperature = 200 °C. Reproduced from Reference [22]. Copyright 2011, with Permission from Elsevier.

They also investigated the influence of Ni loading on the activity of Mn/TiO_2 catalyst, and found that the 5wt%Mn-2wt%Ni/ TiO_2 ($\text{Mn-Ni}(0.4)/\text{TiO}_2$, where $\text{Ni}/\text{Mn} = 0.4$) had the optimal activity with complete NO conversion at the temperature range of 200–250 °C (Figure 19a) and outstanding stability even in the presence of 10 vol% water (Figure 19b,c) [5,23]. The enhanced reducibility of manganese oxide and dominant phase of MnO_2 claimed to be responsible for the best activity and stability of $\text{Mn-Ni}/\text{TiO}_2$ catalyst [5,22,23]. In another study, they compared the de- NO_x performance of high surface texture hydrated titania and Hombikat TiO_2 supported Mn-Ce bimetallic catalysts, and observed that the $\text{Mn-Ce}/\text{TiO}_2$ (Hombikat) showed the better activity and excellent resistance to H_2O (Figure 20). The superior performance could be attributed to the enhancement in reduction potential of active components, broadening of acid sites distribution, and the promotion of $\text{Mn}^{4+}/\text{Mn}^{3+}$, $\text{Ce}^{3+}/\text{Ce}^{4+}$ ratios including surface labile oxygen and small pore openings [25].

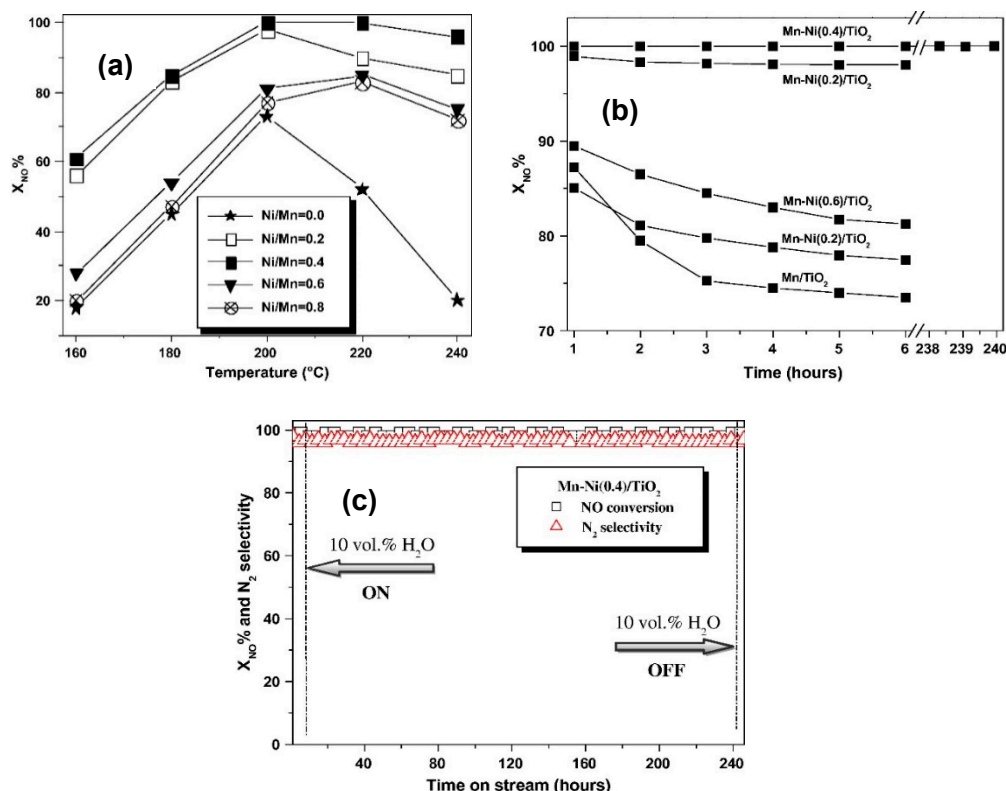


Figure 19. (a) Influence of Ni/Mn atomic ratio on NO conversion in the SCR reaction at a temperature range (160–240 $^{\circ}C$) over Mn-Ni/TiO₂ catalysts ($X_{NO}\%$ = conversion of NO at 6 h on stream); (b) SCR of NO with NH_3 at 200 $^{\circ}C$ temperature over Mn/TiO₂ and Mn-Ni/TiO₂ catalysts; (c) Influence of inlet water concentrations (10 vol%) on NO conversion in the SCR reaction over Mn-Ni(0.4)/TiO₂ catalyst at 200 $^{\circ}C$ (GHSV = 50,000 h^{-1} ; feed: NO = 400 ppm, NH_3 = 400 ppm, O_2 = 2 vol%, He carrier gas, catalyst = 0.1 g, total flow = 140 mL min^{-1}). Reprinted from Reference [5]. Copyright 2012, with Permission from Elsevier.

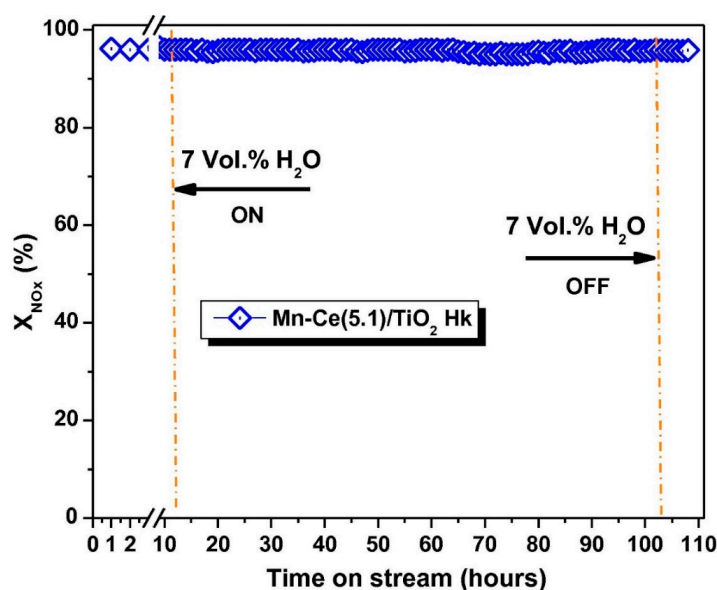


Figure 20. Influence of inlet water concentrations (7 vol%) on NO_x conversion in the SCR reaction over Mn-Ce(5.1)/TiO₂-Hk (Hombikat) catalyst at 175 $^{\circ}C$; feed: NO = 900 ppm, NO₂ = 100 ppm, NH_3/NO_x (ANR) = 1.0, O_2 = 10 vol%, He carrier gas, catalyst = 0.08 g, GHSV = 80,000 h^{-1} . Reprinted from Reference [25]. Copyright 2015, with Permission from Elsevier.

Xu and co-workers [127] reported Ce-Mn/TiO₂ catalysts with different Ce loadings, and the Ce(20)-Mn/TiO₂ found to show high activity with >90% NO conversion in the temperature range of 140–260 °C (Figure 21a). Their SO₂ tolerance results showed that the resistance ability was decreased in the order of Ce(20)-Mn/TiO₂ > Ce(30)-Mn/TiO₂ > Ce(10)-Mn/TiO₂ (Figure 21b). Although the Ce(20)-Mn/TiO₂ catalyst had reasonable resistance to 100 ppm SO₂ at different reaction temperatures (Figure 21c), it exhibited moderate tolerance to SO₂ poisoning when added higher than 100 ppm SO₂ to the reaction feed (Figure 21d). They ascribed the good SO₂ resistance of Ce(20)-Mn/TiO₂ to the widely distributed elements of Mn and Ce which in turn led to the inability of the sulfate material to remain on the surface.

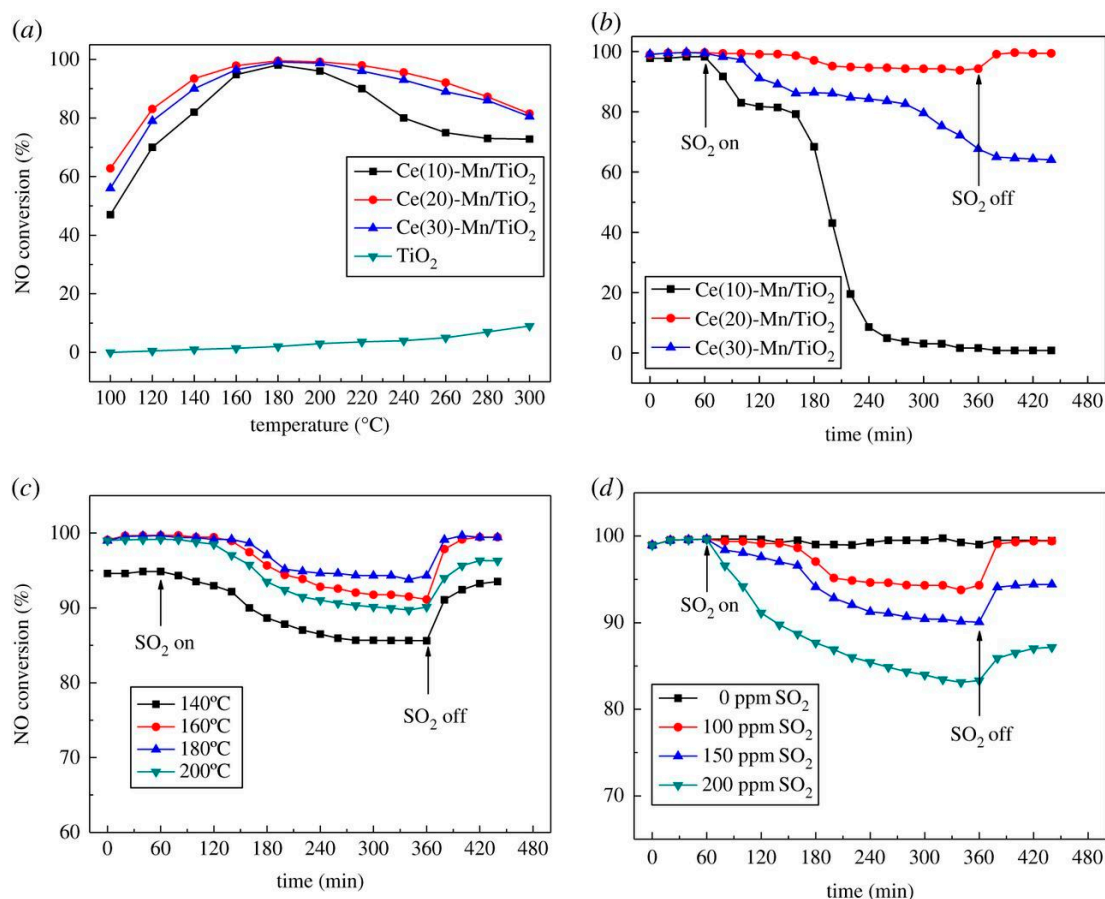


Figure 21. (a) Catalytic activity of Ce-Mn/TiO₂ catalyst for NH₃-SCR. Catalysts were loaded with 10%, 20% and 30% Ce and denoted as Ce(10), Ce(20) and Ce(30), respectively. Pure TiO₂ was also used for comparison; (b) The effect of various Ce concentrations using a Ce-Mn/TiO₂ catalyst on SO₂ resistance; (c) The effects of reaction temperature on NO conversion of the Ce(20)-Mn/TiO₂ catalyst in the presence of SO₂. The above three types of reactions were performed at: 500 ppm NO, 500 ppm NH₃, SO₂ 100 ppm, 3% O₂, N₂ balance. gas, GHSV = 10 000 h⁻¹; and (d) the effects of SO₂ concentration on NO conversion of Ce(20)-Mn/TiO₂ catalysts (T = 180 °C, 500 ppm NO, 500 ppm NH₃, 3% O₂, N₂ balance gas, GHSV = 10 000 h⁻¹). Adapted from Reference [127]. We thank the Royal Society Open Science for this Contribution.

Lin et al. [128] synthesized Me-Fe/TiO₂ (SD) catalyst via an aerosol-assisted deposition method, showing an excellent NH₃-SCR performance and good tolerance to SO₂/H₂O as compared to its counterparts prepared by co-precipitation and wet impregnation methods. The authors concluded that the enhanced surface reducibility and adsorption ability of NH₃/NO_x of Mn-Fe/TiO₂ (SD) catalyst could be responsible for its superior activity. Lee and co-workers [129] investigated the poisoning effect of SO₂ as metal sulfate and/or ammonium sulfate deposits on the low-temperature

NH₃-SCR activity of MnFe/TiO₂ catalysts. They found that the metal sulfates had a more serious deactivation effect than that of ammonium salts on the MnFe/TiO₂ catalysts. Their results showed that metal sulfates poisoning resulted in lower crystallinity, lower specific surface area, a lower ratio of Mn⁴⁺/Mn³⁺, higher surface acidity, and more chemisorbed oxygen, which in turn led to an adverse effect on the NH₃-SCR activity of the catalyst. Mu et al. [130] prepared Fe-Mn/Ti catalyst by ethylene glycol-assisted impregnation method, showing high NH₃-SCR efficiency over a broad temperature window (100–325 °C) and outstanding tolerance to sulfur poisoning. The formation of the Fe-O-Ti structure with strong interaction strengthened the electronic inductive effect and increased the ratio of surface chemisorption oxygen, thereby the enhancement of NO_x adsorption capacity and NO oxidation performance, which could be beneficial to improve the NH₃-SCR activity.

Liu and co-workers [131] reported that the addition of Eu had noticeably improved the NH₃-SCR performance of Mn/TiO₂ catalyst even after sulfation process under SCR conditions (Figure 22a). However, both the Mn/TiO₂ and MnEu/TiO₂ catalysts showed poor activity when they sulfated only with SO₂ + O₂ (Figure 22a). Further, the MnEu/TiO₂ catalyst found to show better SO₂ tolerance as compared to the Mn/TiO₂ (Figure 22b). Their results revealed that Eu modification could inhibit the formation of surface sulfate species on the Mn/TiO₂ catalyst during the NH₃-SCR in the presence of SO₂, which could be the reason for improved SO₂ resistance.

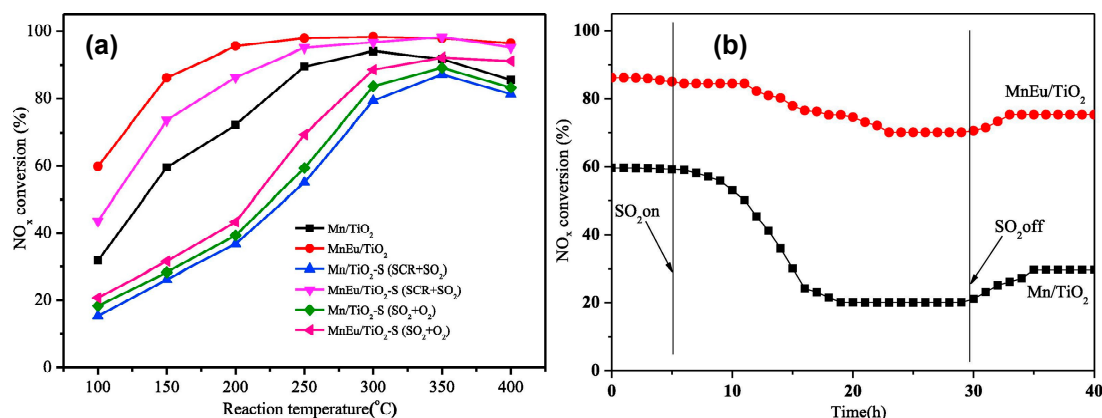


Figure 22. (a) NH₃-SCR activities of the fresh and sulfated catalysts; and (b) SO₂ tolerances of Mn/TiO₂ and MnEu/TiO₂ in NH₃-SCR reaction. Reprinted from Reference [131]. Copyright 2018, with Permission from Elsevier.

Sun et al. [132] investigated the NH₃-SCR activity over the Nb-doped Mn/TiO₂ catalysts with different Nb/Mn molar ratios, and found that the MnNb/TiO₂-0.12 (where Nb/Mn = 0.12) catalyst had optimal NO_x conversion and N₂ selectivity in the temperature range of 100–400 °C (Figure 23a,b). The optimal MnNb/TiO₂-0.12 catalyst also exhibited greater SO₂ resistance than Mn/TiO₂ catalyst (Figure 23c). The incorporation of Nb into Mn/TiO₂ catalyst led to increase surface acidity and reducibility as well as generate more surface Mn⁴⁺ and chemisorbed oxygen species along with more NO₂, which results in the better NH₃-SCR activity. In situ DRIFT studies over the Mn/TiO₂ and MnNb/TiO₂-0.12 catalysts disclosed that the NH₃-SCR took place through Eley–Rideal mechanism even in presence of SO₂, in which the reaction mainly occurred between adsorbed NO₂ and gaseous NH₃. Hence, it was concluded that the higher SO₂ tolerance of the MnNb/TiO₂-0.12 catalyst could be due to the existence of more adsorbed NO₂ on its surface.

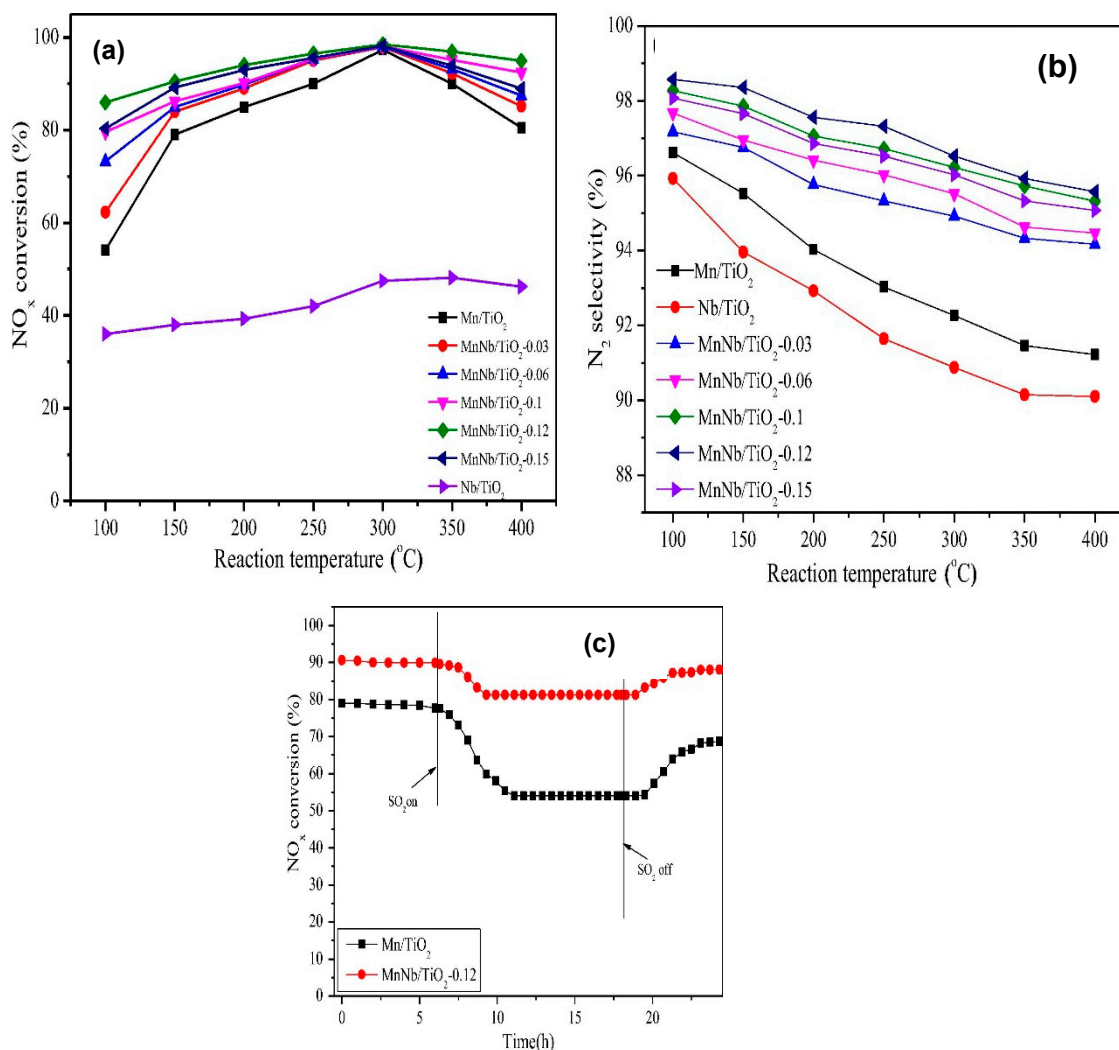


Figure 23. (a) SCR activities and (b) N₂ selectivities over different catalyst samples as a function of reaction temperature. Reaction conditions: [NO] = [NH₃] = 600 ppm, [O₂] = [H₂O] = 5%, balance Ar, GHSV = 108,000 h⁻¹; (c) Effect of SO₂ on the SCR activities over Mn/TiO₂ and MnNb/TiO₂-0.12 catalyst samples. Reaction conditions: [NO] = [NH₃] = 600 ppm, [O₂] = [H₂O] = 5%, [SO₂] = 100 ppm, balance Ar, GHSV = 108,000 h⁻¹, reaction temperature = 150 °C. Reproduced from Reference [132]. Copyright 2018, with Permission from Elsevier.

In another study, they reported the Mo-modified Mn/TiO₂ catalysts, exhibiting improved NH₃-SCR activity from 50 to 400 °C in comparison to Mn/TiO₂ catalyst. Particularly, the optimal MnMo/TiO₂-0.04 (where molar ratio of Mo/Mn = 0.04) catalyst better tolerance to SO₂ poisoning compared with Mn/TiO₂ (Figure 24) [133].

Fan and co-workers [134] fabricated ordered mesoporous titania supported CuO and MnO₂ composites (CuO/MnO₂-mTiO₂) through a facile acetic acid-assisted one-pot synthesis approach, showing high deNO_x efficiency (>90% NO conversion) and N₂ selectivity (>95%) in a wide operating temperature range of 120–300 °C. They considered that the superior NH₃-SCR performance could be attributed to the unique structure and highly integrated mesoporous TiO₂ supported by the multicomponent system with high surface areas, accessible and homogeneously dispersed CuO and MnO₂ with multivalent nature and good redox activity. Although the CuO/MnO₂-mTiO₂ catalyst had good tolerance to H₂O, the resistance to SO₂ and H₂O/SO₂ poisoning, as well as high space velocity (GHSV), still need to be enhanced for practical use. Li et al. [135] synthesized fly ash-derived SBA-15 mesoporous molecular sieves supported Fe and/or Mn catalysts, and reported that Fe-Mn/SBA-15

catalyst showed notably greater NH_3 -SCR activity than $\text{Mn}/\text{SBA-15}$ or $\text{Fe}/\text{SBA-15}$ in the temperature range of 150–250 °C. Moreover, the $\text{Fe-Mn}/\text{SBA-15}$ catalyst exhibited good time-on-stream stability (200 h) and water tolerance at 200 °C. The high metal dispersion, $\text{Mn}^{4+}/\text{Mn}^{3+}$ ratio, the concentration of adsorbed oxygen, and the redox activity are important features to enhance the NH_3 -SCR performance of the $\text{Fe-Mn}/\text{SBA-15}$ catalyst. In their subsequent study, the authors investigated the mechanisms of NO reduction and N_2O formation using in-situ DRIFT and transient reaction studies and proposed a possible denitration mechanism over the $\text{Fe-Mn}/\text{SBA-15}$ catalyst which is shown in Figure 25. The NH_3 -SCR reaction over the $\text{Fe-Mn}/\text{SBA-15}$ catalyst proceeded through Langmuir-Hinshelwood, Eley-Rideal, and Mars-van Krevelen mechanisms. Their results also revealed that a large amount of nitrate thereby N_2O being produced over the $\text{Fe-Mn}/\text{SBA-15}$ during the reaction due to its strong oxidation ability, low acidity, and high basicity, which resulted in the lower N_2 selectivity [136].

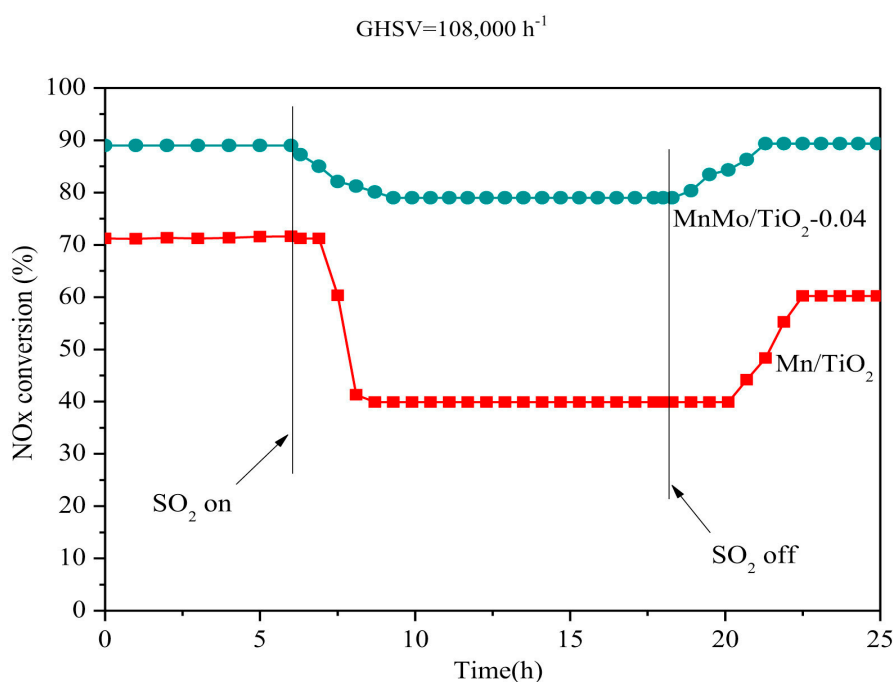


Figure 24. SO_2 tolerance of Mn/TiO_2 and $\text{MnMo}/\text{TiO}_2\text{-0.04}$ catalysts at 150 °C, Reaction conditions: 600 ppm NO, 600 ppm NH_3 , 100 ppm SO_2 , 5% O_2 , balance Ar, GHSV = 108,000 h^{-1} . Reprinted from Reference [133]. Copyright 2018, with Permission from Elsevier.

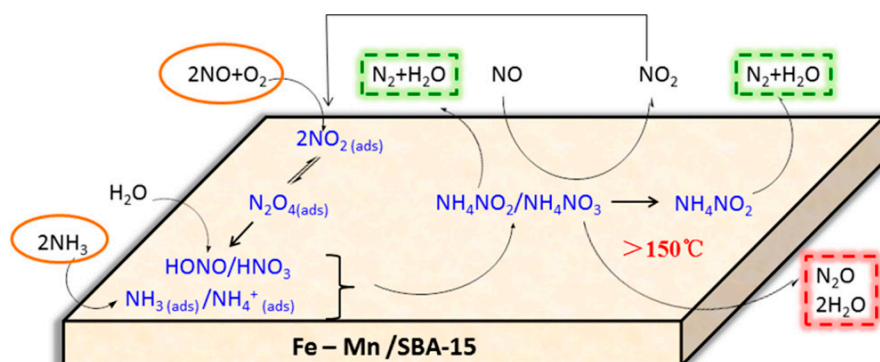


Figure 25. Low-temperature NH_3 -SCR reaction mechanism on $\text{Fe-Mn}/\text{SBA-15}$ catalyst. Adapted from Reference [136]. Copyright 2018, with Permission from American Chemical Society.

Tang and co-workers [137] reported that $\text{Mn}_2\text{CoO}_4/\text{reduced graphene oxide}$ ($\text{Mn}_2\text{CoO}_4/\text{rGO}$) catalyst with an optimal amount of $\text{CoCl}_2 \cdot 6\text{H}_2\text{O}$ of 0.3 (millimole) showed excellent NH_3 -SCR activity and stability at low-temperature due to its large specific surface area, abundant Lewis acid sites,

and special three-dimensional architecture. When 100 ppm SO₂ added to reaction feed, the NO_x conversion over the optimal catalyst decreased significantly (96% to 53%), and the NO_x conversion was recovered to original level by water-washing after stopping the supply of SO₂. However, the decreased activity (100% to 82% NO_x conversion) in the presence of H₂O was restored to the original level after removing H₂O from the feed gas. Wang et al. [138] investigated the honeycomb cordierite-based Mn-Ce/Al₂O₃ catalyst for NH₃-SCR reaction and found that it showed good activity and reasonable resistance to SO₂/H₂O. The catalyst deactivation in the presence of SO₂ was ascribed to the deposition of ammonium hydrogen sulfate and sulfated CeO₂ on the catalyst surface during the NH₃-SCR process.

Meng et al. [139] synthesized a novel CuAlO_x/CNTs (CNTs = carbon nanotubes) catalyst by facile one-step carbothermal reduction decomposition method for low-temperature NH₃-SCR. The CuAlO_x/CNTs catalyst was found to exhibit higher NO_x conversion (>80%) and N₂ selectivity (>90%) than the CuAlO_x in the temperature range of 180–300 °C (Figure 26a). They concluded that more favorable formation of Cu⁺ active sites, better dispersion of active CuO species and higher surface adsorbed oxygen were beneficial to enhance the NH₃-SCR activity of CuAlO_x/CNTs catalyst. As shown in Figure 26b, the CuAlO_x/CNTs catalyst displayed excellent resistance to SO₂/H₂O at 240 °C during the NH₃-SCR. The authors attributed this outstanding SO₂/H₂O tolerance to the presence of CNTs that could promote the reaction of NH₄HSO₄ and NO continuously to avoid the formation and accumulation of excess ammonium sulfate salts on the catalyst surface. Li group [140] reported a series of ultra-low content copper-modified TiO₂/CeO₂ catalysts and observed that the catalyst with a Cu/Ce molar ratio of 0.005 exhibited the high NH₃-SCR performance and good tolerance to SO₂. Their characterization results disclosed that the addition of Cu into TiO₂/CeO₂ lead to enhance the Brønsted acid sites, amount of surface adsorbed oxygen and Ce³⁺ species, redox, and surface acidic properties, which in turn improve the NH₃-SCR activity.

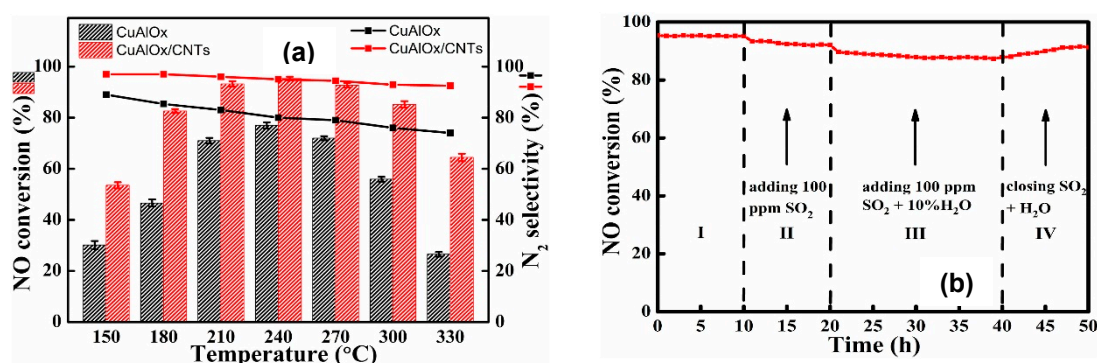


Figure 26. (a) NH₃-SCR activity and N₂ selectivity as a function of temperature from 150 °C to 330 °C; and (b) SO₂/H₂O resistance test of CuAlO_x/CNTs catalyst at 240 °C. Reaction conditions: 600 ppm NH₃, 600 ppm NO, 5.0 vol% O₂, 100 ppm SO₂ (when used), 10 vol% H₂O (when used) balanced by N₂ with a GHSV was 45,000 h⁻¹. Reprinted from Reference [139]. Copyright 2019, with Permission from Elsevier.

Recently, supported multi-metal oxide catalysts have been considered as the very promising candidates for low-temperature NH₃-SCR reaction because of the enlarged synergetic catalysis effects of different components as well as improved metal-support interactions [141–145]. Wang and co-workers [146] reported a series of Nb modified Cu-Ce-Ti mixed oxide (Nb_yCCT, where y represented the atomic ratio of Nb to Ti) catalysts for low-temperature NH₃-SCR reaction. It was found that Nb_yCCT catalysts demonstrated a better activity than the Cu-Ce-Ti (CCT) and Ce-Ti (CT) samples (Figure 27a). Among all the Nb_yCCT catalysts, Nb_{0.05}CCT showed a higher NO conversion (>90%) in a broad temperature range of 180–360 °C under the GHSV of 40,000 h⁻¹ (Figure 27a). Results indicated that the incorporation of Nb to Cu-Ce-Ti led to strong interactions among the active phases that increased the oxygen vacancies and inhibited the over-oxidation of NH₃, which in turn improved the NH₃-SCR activity and N₂ selectivity in a wide temperature window. DRIFTS studies revealed

that the introduction of Nb promoted the generation of NO_2 , which could improve the activity via “fast” SCR reaction process (Langmuir–Hinshelwood reaction pathway). As shown in Figure 27b, the optimal $\text{Nb}_{0.05}\text{CCT}$ catalyst exhibited higher resistance to $\text{SO}_2/\text{H}_2\text{O}$ as compared to the Nb free catalyst. Li et al. [147] investigated the effect of Ho doping on the NH_3 -SCR performance and the $\text{SO}_2/\text{H}_2\text{O}$ resistance of Mn-Ce/ TiO_2 catalyst. Among the catalysts tested, the catalyst with Ho/Ti of 0.1 ($\text{Mn}_{0.4}\text{Ce}_{0.07}\text{Ho}_{0.1}/\text{TiO}_2$) showed the best performance with >90% NO conversion in the temperature range of 150–220 °C, which was attributed to high concentration of chemisorbed oxygen, surface $\text{Mn}^{4+}/\text{Mn}^{3+}$ ratio, and acidity, as well as large specific surface area. Although the $\text{Mn}_{0.4}\text{Ce}_{0.07}\text{Ho}_{0.1}/\text{TiO}_2$ showed higher resistance to SO_2 and H_2O than the $\text{Mn}_{0.4}\text{Ce}_{0.07}/\text{TiO}_2$ catalyst, it was deactivated some extent in presence of $\text{SO}_2/\text{H}_2\text{O}$ which is irreversible.

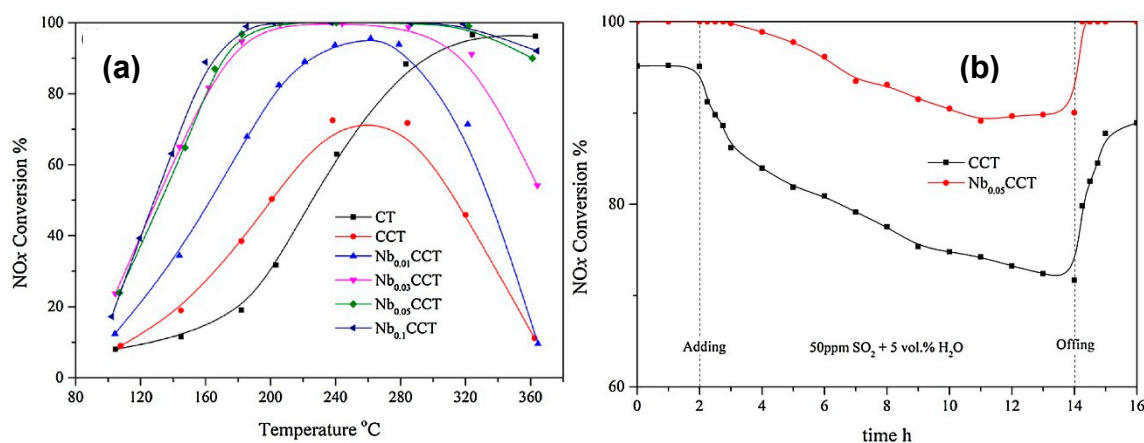


Figure 27. (a) NH_3 -SCR activities of different catalysts {Reaction conditions: $[\text{NH}_3] = [\text{NO}] = 600$ ppm, $[\text{O}_2] = 3\%$, $[\text{H}_2\text{O}] = 5$ vol%, N_2 as balance. GHSV = $40\,000\text{ h}^{-1}$ }; and (b) SO_2 and H_2O resistance of the catalysts at 250 °C in SCR reaction process [Reaction conditions: $[\text{NH}_3] = [\text{NO}] = 600$ ppm, $[\text{O}_2] = 3\%$, $[\text{SO}_2] = 50$ ppm, $[\text{H}_2\text{O}] = 5$ vol%, N_2 balance, GHSV = $40\,000\text{ h}^{-1}$]. Reproduced from Reference [146]. Copyright 2018, with Permission from Elsevier.

Lu group [148] synthesized a series of activated coke (AC) supported $\text{Fe}_x\text{Co}_y\text{Ce}_z\text{O}_m$ catalysts for low-temperature NH_3 -SCR, and found that the 3% $\text{Fe}_{0.6}\text{Co}_{0.2}\text{Ce}_{0.2}\text{O}_{1.57}/\text{AC}$ catalyst had the best activity at 250–350 °C and good tolerance to $\text{H}_2\text{O}/\text{SO}_2$ at 250 °C. The superior performance of the catalyst was ascribed to the co-participation of Fe, Co, and Ce species with different valence states, high concentration of chemisorbed oxygen, well dispersed active components, increase of weak acid sites, good redox properties of metallic oxides, and abundant functional groups on the catalyst surface. Their mechanistic and kinetic studies also indicated that the enhanced active sites for the adsorption of NO and NH_3 , and the redox cycle among Fe, Co and Ce were responsible for the improved activity. Zhao et al. [149] reported a series of Mn-Ce-V- WO_x/TiO_2 composite oxide catalysts, exhibiting greater NH_3 -SCR activity than the TiO_2 supported single-component catalysts (Figure 28a,b). Particularly, the catalyst with a molar ratio of active components/ $\text{TiO}_2 = 0.2$ showed the best performance (>90% NO conversion) from 150 to 400 °C (Figure 28a). As shown in Figure 28c, the optimal Mn-Ce-V- WO_x/TiO_2 (molar ratio of Mn-Ce-V- $\text{WO}_x/\text{TiO}_2 = 0.2$) showed excellent stability and outstanding tolerance to $\text{H}_2\text{O}/\text{SO}_2$ at 250 °C. The authors concluded that the better performance of Mn-Ce-V- WO_x/TiO_2 mainly attributed to the variety of valence states of the four active components and their high oxidation-reduction ability.

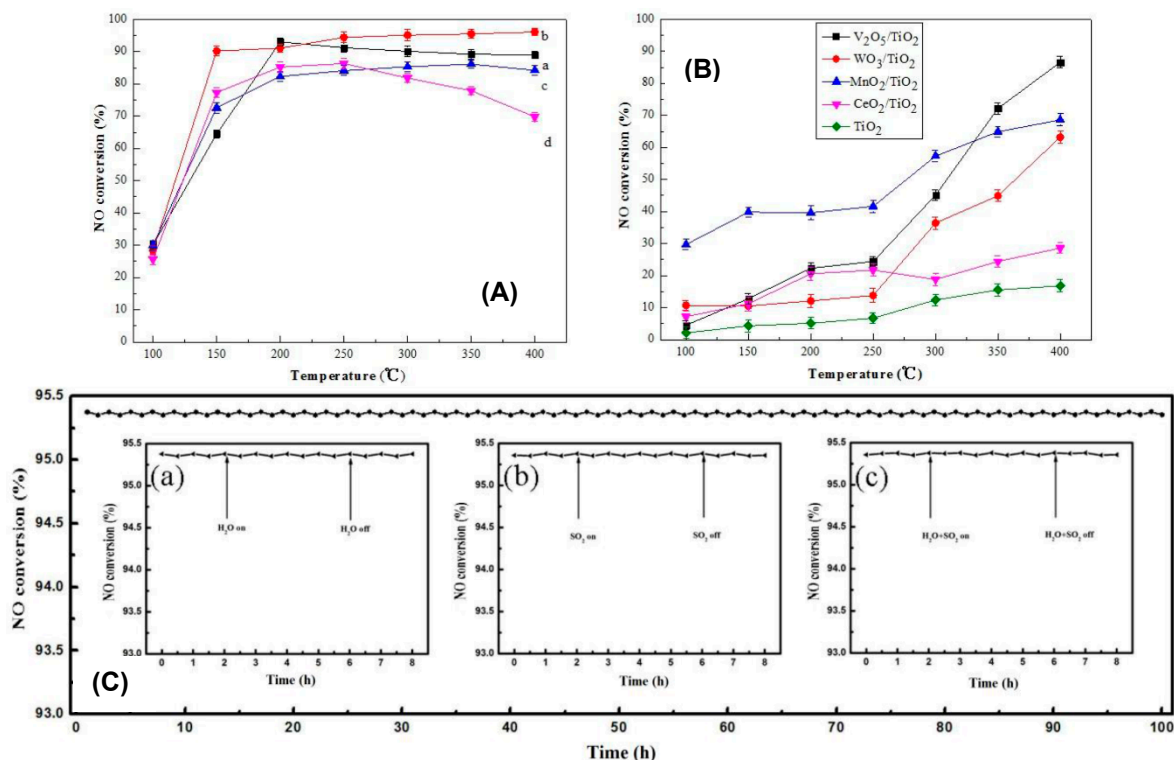


Figure 28. (A) Selective catalytic reduction (SCR) activity of Mn-Ce-V-WO_x/TiO₂ composite catalysts with molar ratio of active components/TiO₂ at different values; (a) 0.1; (b) 0.2; (c) 0.3; (d) 0.6; (B) SCR activity of V₂O₅/TiO₂, WO₃/TiO₂, MnO₂/TiO₂, CeO₂/TiO₂ and TiO₂. Reaction conditions: [NO] = [NH₃] = 1500 ppm, O₂ = 3%, gas hourly space velocity (GHSV) = 40,000 h⁻¹; and (C) the lifetime of Mn-Ce-V-WO_x/TiO₂ catalyst with molar ratio of 0.2 at 250 °C: inset (a-c) H₂O and SO₂ resistance at 250 °C. Reaction conditions: [NO] = [NH₃] = 1500 ppm, [O₂] = 3%, [H₂O] = 5%, [SO₂] = 100 ppm, GHSV = 40,000 h⁻¹. Adapted from Reference [149].

6. Conclusions

Since the emission standards for NO_x are becoming more stringent to keep our atmosphere clean, the widespread use of fossil fuel in automobiles and industries require advanced catalytic materials for NO_x emission control. The low-temperature SCR of NO_x with NH₃ would be a promising solution to mitigate the NO_x emissions from mobile and stationary sources. Hence, the development of efficient catalysts for the low-temperature NH₃-SCR with high deNO_x activity, N₂ selectivity, and high resistance toward SO₂/H₂O poisonings is the subject of increasing interest in the field of environmental catalysis. Transition metal-based oxide catalysts have drawn much attention for low-temperature NH₃-SCR due to their excellent redox properties, high activity, durability, and relatively low manufacturing costs. In this review, we have summarized the recent progress in the low-temperature NH₃-SCR technology over the various transition metal-based catalysts. Over the past decades, significant research efforts have been made to improve the de-NO_x efficiency and SO₂/H₂O tolerance of transition metal-based oxides in NH₃-SCR at low-temperatures. Various transition metal-based mixed oxides with and without support have been extensively studied for NH₃-SCR reaction and, particularly, MnO_x-based catalyst formulations have caught much attention because of their excellent de-NO_x efficiency at low-temperatures. The modification of transition metal oxides by doping with other metal oxides led to high redox ability and acidic sites, and consequently, better NH₃-SCR performance at low-temperature. The loading of single and multi-transition metal-based oxides on the surface of supports (TiO₂, TiO₂ nanotubes, carbon nanotubes, etc.) could also enhance the NO_x conversion and N₂ selectivity in NH₃-SCR reaction by the fine dispersion of active component/s and its/their strong interaction with the support. The choice of metal loading and the support

could play a key role in the catalytic function of the supported transition metal-based catalysts. The synergistic redox interaction between the active components of mixed metal oxide/supported metal oxide catalysts was also found to be an important factor to design the efficient denitration catalysts. In spite of the significant progress on the SO₂/H₂O tolerance of the catalysts, the durability of catalysts in the presence of both SO₂ and H₂O still needs to be improved. Most transition metal-based catalysts suffered from low resistance when the reaction feed contains both SO₂ and H₂O streams simultaneously. Hence, researchers have continuously explored the different options of transition metal-based mixed oxides and active transition metal/s-support combinations in order to develop the better NH₃-SCR catalysts in terms of SO₂/H₂O tolerance at low-temperature. The understanding of the inhibition mechanism of SO₂ and H₂O could be a promising strategy to develop high SO₂/H₂O resistance catalysts for NH₃-SCR reaction. However, the SO₂/H₂O inhibition mechanism was not very clear that needs to be investigated deeply. Especially, the design of transition metal-based catalysts with a combination of high NO_x conversion and N₂ selectivity in a wide operation temperature window and good resistance to SO₂/H₂O have attracted paramount attention, but it is still challenging task. The scope of NH₃-SCR research is quite vast and a large number of improvements need to be achieved in the near future.

Author Contributions: The original draft was prepared by D.D., reviewed and edited by D.D., P.G.S., B.M.R. and P.R.E.

Funding: This research received no external funding.

Conflicts of Interest: The authors declare no conflict of interest.

References

1. Wan, Y.; Zhao, W.; Tang, Y.; Li, L.; Wang, H.; Cui, Y.; Gu, J.; Li, Y.; Shi, J. Ni-Mn bi-metal oxide catalysts for the low temperature SCR removal of NO with NH₃. *Appl. Catal. B* **2014**, *148–149*, 114–122. [[CrossRef](#)]
2. Boningari, T.; Smirniotis, P.G. Impact of nitrogen oxides on the environment and human health: Mn-based materials for the NO_x abatement. *Curr. Opin. Chem. Eng.* **2016**, *13*, 133–141. [[CrossRef](#)]
3. Xin, Y.; Li, Q.; Zhang, Z. Zeolitic materials for DeNO_x selective catalytic reduction. *ChemCatChem* **2018**, *10*, 29–41. [[CrossRef](#)]
4. Damma, D.; Boningari, T.; Ettireddy, P.R.; Reddy, B.M.; Smirniotis, P.G. Direct decomposition of NO_x over TiO₂ supported transition metal oxides at low temperatures. *Ind. Eng. Chem. Res.* **2018**, *57*, 16615–16621. [[CrossRef](#)]
5. Thirupathi, B.; Smirniotis, P.G. Nickel-doped Mn/TiO₂ as an efficient catalyst for the low-temperature SCR of NO with NH₃: Catalytic evaluation and characterizations. *J. Catal.* **2012**, *288*, 74–83. [[CrossRef](#)]
6. Chen, L.; Si, Z.; Wu, X.; Weng, D. DRIFT study of CuO–CeO₂–TiO₂ mixed oxides for NO_x reduction with NH₃ at low temperatures. *ACS Appl. Mater. Interfaces* **2014**, *6*, 8134–8145. [[CrossRef](#)]
7. Chen, M.; Yang, J.; Liu, Y.; Li, W.; Fan, J.; Ran, X.; Teng, W.; Sun, Y.; Zhang, W.-X.; Li, G.; et al. TiO₂ interpenetrating networks decorated with SnO₂ nanocrystals: Enhanced activity of selective catalytic reduction of NO with NH₃. *J. Mater. Chem. A* **2015**, *3*, 1405–1409. [[CrossRef](#)]
8. Chen, Z.; Yang, Q.; Li, H.; Li, X.; Wang, L.; Tsang, S.C. Cr–MnO_x mixed-oxide catalysts for selective catalytic reduction of NO_x with NH₃ at low temperature. *J. Catal.* **2010**, *276*, 56–65. [[CrossRef](#)]
9. Boningari, T.; Koirala, R.; Smirniotis, P.G. Low-temperature selective catalytic reduction of NO with NH₃ over V/ZrO₂ prepared by flame-assisted spray pyrolysis: Structural and catalytic properties. *Appl. Catal. B* **2012**, *127*, 255–264. [[CrossRef](#)]
10. Chen, L.; Li, J.; Ge, M. DRIFT study on cerium-tungsten/titania catalyst for selective catalytic reduction of NO_x with NH₃. *Environ. Sci. Technol.* **2010**, *44*, 9590–9596. [[CrossRef](#)]
11. Liu, F.; Asakura, K.; He, H.; Shan, W.; Shi, X.; Zhang, C. Influence of sulfation on iron titanate catalyst for the selective catalytic reduction of NO_x with NH₃. *Appl. Catal. B* **2011**, *103*, 369–377. [[CrossRef](#)]
12. Cai, S.; Zhang, D.; Zhang, L.; Huang, L.; Li, H.; Gao, R.; Shi, L.; Zhang, J. Comparative study of 3D ordered macroporous Ce_{0.75}Zr_{0.2}M_{0.05}O_{2–δ} (M = Fe, Cu, Mn, Co) for selective catalytic reduction of NO with NH₃. *Catal. Sci. Technol.* **2014**, *4*, 93–101. [[CrossRef](#)]

13. Wang, X.; Wen, W.; Su, Y.; Wang, R. Influence of transition metals (M = Co, Fe and Mn) on ordered mesoporous CuM/CeO₂ catalysts and applications in selective catalytic reduction of NO_x with H₂. *RSC Adv.* **2015**, *5*, 63135–63141. [[CrossRef](#)]
14. Liu, J.; Li, X.; Zhao, Q.; Ke, J.; Xiao, H.; Lv, X.; Liu, S.; Tadé, M.; Wang, S. Mechanistic investigation of the enhanced NH₃-SCR on cobalt-decorated Ce-Ti mixed oxide: In situ FTIR analysis for structure-activity correlation. *Appl. Catal. B* **2017**, *200*, 297–308. [[CrossRef](#)]
15. Schneider, H.; Maciejewski, M.; Köhler, K.; Wokaun, A.; Baiker, A. Chromia supported on titania, VI Properties of different chromium oxide phases in the catalytic reduction of NO by NH₃ studied by in situ diffuse reflectance FTIR spectroscopy. *J. Catal.* **1995**, *157*, 312–320. [[CrossRef](#)]
16. Chen, Z.; Wang, F.; Li, H.; Yang, Q.; Wang, L.; Li, X. Low-temperature selective catalytic reduction of NO_x with NH₃ over Fe-Mn mixed-oxide catalysts containing Fe₃Mn₃O₈ phase. *Ind. Eng. Chem. Res.* **2012**, *51*, 202–212. [[CrossRef](#)]
17. Smirniotis, P.G.; Peña, D.A.; Uphade, B.S. Low-temperature selective catalytic reduction (SCR) of NO with NH₃ by using Mn, Cr, and Cu oxides supported on hombikat TiO₂. *Angew. Chem. Int. Ed.* **2001**, *40*, 2479–2482. [[CrossRef](#)]
18. Wu, Z.; Jiang, B.; Liu, Y. Effect of transition metals addition on the catalyst of manganese/titania for low-temperature selective catalytic reduction of nitric oxide with ammonia. *Appl. Catal. B* **2008**, *79*, 347–355. [[CrossRef](#)]
19. Liu, F.; He, H.; Zhang, C.; Feng, Z.; Zheng, L.; Xie, Y.; Hu, T. Selective catalytic reduction of NO with NH₃ over iron titanate catalyst: Catalytic performance and characterization. *Appl. Catal. B* **2010**, *96*, 408–420. [[CrossRef](#)]
20. Yao, X.; Kong, T.; Chen, L.; Ding, S.; Yang, F.; Dong, L. Enhanced low-temperature NH₃-SCR performance of MnO_x/CeO₂ catalysts by optimal solvent effect. *Appl. Surf. Sci.* **2017**, *420*, 407–415. [[CrossRef](#)]
21. Sreekanth, P.M.; Peña, D.A.; Smirniotis, P.G. Titania supported bimetallic transition metal oxides for low-temperature SCR of NO with NH₃. *Ind. Eng. Chem. Res.* **2006**, *45*, 6444–6449. [[CrossRef](#)]
22. Thirupathi, B.; Smirniotis, P.G. Co-doping a metal (Cr, Fe, Co, Ni, Cu, Zn, Ce, and Zr) on Mn/TiO₂ catalyst and its effect on the selective reduction of NO with NH₃ at low-temperatures. *Appl. Catal. B* **2011**, *110*, 195–206. [[CrossRef](#)]
23. Thirupathi, B.; Smirniotis, P.G. Effect of nickel as dopant in Mn/TiO₂ catalysts for the low-temperature selective reduction of NO with NH₃. *Catal. Lett.* **2011**, *141*, 1399–1404. [[CrossRef](#)]
24. Ettireddy, P.R.; Ettireddy, N.; Boningari, T.; Pardemann, R.; Smirniotis, P.G. Investigation of the selective catalytic reduction of nitric oxide with ammonia over Mn/TiO₂ catalysts through transient isotopic labeling and in situ FT-IR studies. *J. Catal.* **2012**, *292*, 53–63. [[CrossRef](#)]
25. Boningari, T.; Ettireddy, P.R.; Somogyvari, A.; Liu, Y.; Vorontsov, A.; McDonald, C.A.; Smirniotis, P.G. Influence of elevated surface texture hydrated titania on Ce-doped Mn/TiO₂ catalysts for the low-temperature SCR of NO_x under oxygen-rich conditions. *J. Catal.* **2015**, *325*, 145–155. [[CrossRef](#)]
26. Pappas, D.K.; Boningari, T.; Boolchand, P.; Smirniotis, P.G. Novel manganese oxide confined interweaved titania nanotubes for the low-temperature selective catalytic reduction (SCR) of NO_x by NH₃. *J. Catal.* **2016**, *334*, 1–13. [[CrossRef](#)]
27. Yu, J.; Guo, F.; Wang, Y.; Zhu, J.; Liu, Y.; Su, F.; Gao, S.; Xu, G. Sulfur poisoning resistant mesoporous Mn-base catalyst for low-temperature SCR of NO with NH₃. *Appl. Catal. B* **2010**, *95*, 160–168. [[CrossRef](#)]
28. Cai, S.; Zhang, D.; Shi, L.; Xu, J.; Zhang, L.; Huang, L.; Li, H.; Zhang, J. Porous Ni–Mn oxide nanosheets in situ formed on nickel foam as 3D hierarchical monolith de-NO_x catalysts. *Nanoscale* **2014**, *6*, 7346–7353. [[CrossRef](#)] [[PubMed](#)]
29. Zhang, S.; Zhang, B.; Liu, B.; Sun, S. A review of Mn-containing oxide catalysts for low temperature selective catalytic reduction of NO_x with NH₃: Reaction mechanism and catalyst deactivation. *RSC Adv.* **2017**, *7*, 26226–26242. [[CrossRef](#)]
30. Zhang, L.; Shi, L.; Huang, L.; Zhang, J.; Gao, R.; Zhang, D. Rational design of high-performance DeNO_x catalysts based on Mn_xCo_{3-x}O₄ nanocages derived from metal–organic frameworks. *ACS Catal.* **2014**, *4*, 1753–1763. [[CrossRef](#)]

31. Li, L.; Wu, Y.; Hou, X.; Chu, B.; Nan, B.; Qin, Q.; Fan, M.; Sun, C.; Li, B.; Dong, L.; et al. Investigation of two-phase intergrowth and coexistence in Mn–Ce–Ti–O catalysts for the selective catalytic reduction of NO with NH₃: Structure–activity relationship and reaction mechanism. *Ind. Eng. Chem. Res.* **2019**, *58*, 849–862. [[CrossRef](#)]
32. Gao, F.; Tang, X.; Yi, H.; Zhao, S.; Wang, J.; Gu, T. Improvement of activity, selectivity and H₂O&SO₂-tolerance of micromesoporous CrMn₂O₄ spinel catalyst for low-temperature NH₃-SCR of NO_x. *Appl. Surf. Sci.* **2019**, *466*, 411–424.
33. Li, X.J.; Du, Y.; Guo, X.M.; Wang, R.N.; Hou, B.H.; Wu, X. Synthesis of a novel NiMnTi mixed metal oxides from LDH precursor and its catalytic application for selective catalytic reduction of NO_x with NH₃. *Catal. Lett.* **2019**, *149*, 456–464. [[CrossRef](#)]
34. Yang, G.; Zhao, H.; Luo, X.; Shi, K.; Zhao, H.; Wang, W.; Chen, Q.; Fan, H.; Wu, T. Promotion effect and mechanism of the addition of Mo on the enhanced low temperature SCR of NO_x by NH₃ over MnO_x/γ-Al₂O₃ catalysts. *Appl. Catal. B* **2019**, *245*, 743–752. [[CrossRef](#)]
35. Wang, X.; Wu, W.; Chen, Z.; Wang, R. Bauxite-supported transition metal oxides: Promising low-temperature and SO₂-tolerant catalysts for selective catalytic reduction of NO_x. *Sci. Rep.* **2015**, *5*, 9766. [[CrossRef](#)]
36. Wang, Z.-Y.; Guo, R.-T.; Shi, X.; Pan, W.-G.; Liu, J.; Sun, X.; Liu, S.-W.; Liu, X.-Y.; Qin, H. The enhanced performance of Sb-modified Cu/TiO₂ catalyst for selective catalytic reduction of NO_x with NH₃. *Appl. Surf. Sci.* **2019**, *475*, 334–341. [[CrossRef](#)]
37. Hu, H.; Cai, S.; Li, H.; Huang, L.; Shi, L.; Zhang, D. Mechanistic aspects of deNO_x processing over TiO₂ supported Co–Mn oxide catalysts: Structure–activity relationships and in situ DRIFTS analysis. *ACS Catal.* **2015**, *5*, 6069–6077. [[CrossRef](#)]
38. Meng, B.; Zhao, Z.; Chen, Y.; Wang, X.; Li, Y.; Qiu, J. Low-temperature synthesis of Mn-based mixed metal oxides with novel fluffy structures as efficient catalysts for selective reduction of nitrogen oxides by ammonia. *Chem. Commun.* **2014**, *50*, 12396–12399. [[CrossRef](#)]
39. Qiu, M.; Zhan, S.; Zhu, D.; Yu, H.; Shi, Q. NH₃-SCR performance improvement of mesoporous Sn modified Cr-MnO_x catalysts at low temperatures. *Catal. Today* **2015**, *258*, 103–111. [[CrossRef](#)]
40. Shi, J.-W.; Gao, C.; Liu, C.; Fan, Z.; Gao, G.; Niu, C. Porous MnO_x for low-temperature NH₃-SCR of NO_x: The intrinsic relationship between surface physicochemical property and catalytic activity. *J. Nanopart. Res.* **2017**, *19*, 194–204. [[CrossRef](#)]
41. Husnain, N.; Wang, E.; Li, K.; Anwar, M.T.; Mehmood, A.; Gul, M.; Li, D.; Mao, J. Iron oxide-based catalysts for low-temperature selective catalytic reduction of NO_x with NH₃. *Rev. Chem. Eng.* **2019**, *35*, 239–264. [[CrossRef](#)]
42. Liu, F.; Shan, W.; Lian, Z.; Xie, L.; Yang, W.; He, H. Novel MnWO_x catalyst with remarkable performance for low temperature NH₃-SCR of NO_x. *Catal. Sci. Technol.* **2013**, *3*, 2699–2707. [[CrossRef](#)]
43. Fan, G.; Shi, J.-W.; Gao, C.; Gao, G.; Wang, B.; Niu, C. Rationally designed porous MnO_x–FeO_x nanoneedles for low-temperature selective catalytic reduction of NO_x by NH₃. *ACS Appl. Mater. Interfaces* **2017**, *9*, 16117–16127. [[CrossRef](#)] [[PubMed](#)]
44. Gao, G.; Shi, J.-W.; Fan, G.; Gao, C.; Niu, C. Mn₂O₄ microspheres (M = Co, Cu, Ni) for selective catalytic reduction of NO with NH₃: Comparative study on catalytic activity and reaction mechanism via in-situ diffuse reflectance infrared Fourier transform spectroscopy. *Chem. Eng. J.* **2017**, *325*, 91–100. [[CrossRef](#)]
45. Gao, F.; Tang, X.; Yi, H.; Zhao, S.; Li, C.; Li, J.; Shi, Y.; Meng, X. A Review on selective catalytic reduction of NO_x by NH₃ over Mn-based catalysts at low temperatures: Catalysts, mechanisms, kinetics and DFT calculations. *Catalysts* **2017**, *7*, 199. [[CrossRef](#)]
46. Gao, C.; Shi, J.-W.; Fan, Z.; Gao, G.; Niu, C. Sulfur and water resistance of Mn-based catalysts for low-temperature selective catalytic reduction of NO_x: A review. *Catalysts* **2018**, *8*, 11. [[CrossRef](#)]
47. Hu, X.; Huang, L.; Zhang, J.; Li, H.; Zha, K.; Shi, L.; Zhang, D. Facile and template-free fabrication of mesoporous 3D nanosphere-like Mn_xCo_{3-x}O₄ as highly effective catalysts for low temperature SCR of NO_x with NH₃. *J. Mater. Chem. A* **2018**, *6*, 2952–2963. [[CrossRef](#)]
48. Meng, D.; Xu, Q.; Jiao, Y.; Guo, Y.; Guo, Y.; Wang, L.; Lu, G.; Zhan, W. Spinel structured Co_aMn_bO_x mixed oxide catalyst for the selective catalytic reduction of NO_x with NH₃. *Appl. Catal. B* **2018**, *221*, 652–663. [[CrossRef](#)]

49. Yan, Q.; Nie, Y.; Yang, R.; Cui, Y.; O'Hare, D.; Wang, Q. Highly dispersed Cu_yAlO_x mixed oxides as superior low-temperature alkali metal and SO_2 resistant NH_3 -SCR catalysts. *Appl. Catal. A* **2017**, *538*, 37–50. [[CrossRef](#)]
50. Meng, D.; Zhan, W.; Guo, Y.; Guo, Y.; Wang, L.; Lu, G. A Highly effective catalyst of Sm-MnO_x for the NH_3 -SCR of NO_x at low temperature: Promotional role of Sm and its catalytic performance. *ACS Catal.* **2015**, *5*, 5973–5983. [[CrossRef](#)]
51. Sun, P.; Guo, R.-T.; Liu, S.-M.; Wang, S.-X.; Pan, W.-G.; Li, M.-Y. The enhanced performance of MnO_x catalyst for NH_3 -SCR reaction by the modification with Eu. *Appl. Catal. A* **2017**, *531*, 129–138. [[CrossRef](#)]
52. Xin, Y.; Li, H.; Zhang, N.; Li, Q.; Zhang, Z.; Cao, X.; Hu, P.; Zheng, L.; Anderson, J.A. Molecular-level insight into selective catalytic reduction of NO_x with NH_3 to N_2 over a highly efficient bifunctional $\text{V}_a\text{-MnO}_x$ catalyst at low temperature. *ACS Catal.* **2018**, *8*, 4937–4949. [[CrossRef](#)]
53. Han, Y.; Mu, J.; Li, X.; Gao, J.; Fan, S.; Tan, F.; Zhao, Q. Triple-shelled NiMn_2O_4 hollow spheres as an efficient catalyst for low-temperature selective catalytic reduction of NO_x with NH_3 . *Chem. Commun.* **2018**, *54*, 9797–9800. [[CrossRef](#)] [[PubMed](#)]
54. Gao, F.; Tang, X.; Yi, H.; Zhao, S.; Wang, J.; Shi, Y.; Meng, X. Novel Co- or Ni-Mn binary oxide catalysts with hydroxyl groups for NH_3 -SCR of NO_x at low temperature. *Appl. Surf. Sci.* **2018**, *443*, 103–113. [[CrossRef](#)]
55. Sun, W.; Li, X.; Zhao, Q.; Mu, J.; Chen, J. Fe-Mn mixed oxide catalysts synthesized by one-step urea-precipitation method for the selective catalytic reduction of NO_x with NH_3 at low temperatures. *Catal. Lett.* **2018**, *148*, 227–234. [[CrossRef](#)]
56. Kwon, D.W.; Nam, K.B.; Hong, S.C. The role of ceria on the activity and SO_2 resistance of catalysts for the selective catalytic reduction of NO_x by NH_3 . *Appl. Catal. B* **2015**, *166–167*, 37–44. [[CrossRef](#)]
57. Fan, G.; Shi, J.-W.; Gao, C.; Gao, G.; Wang, B.; Wang, Y.; He, C.; Niu, C. Gd-modified MnO_x for the selective catalytic reduction of NO by NH_3 : The promoting effect of Gd on the catalytic performance and sulfur resistance. *Chem. Eng. J.* **2018**, *348*, 820–830. [[CrossRef](#)]
58. Li, C.; Tang, X.; Yi, H.; Wang, L.; Cui, X.; Chu, C.; Li, J.; Zhang, R.; Yu, Q. Rational design of template-free $\text{MnO}_x\text{-CeO}_2$ hollow nanotube as de- NO_x catalyst at low temperature. *Appl. Surf. Sci.* **2018**, *428*, 924–932. [[CrossRef](#)]
59. Liu, F.; Yu, Y.; He, H. Environmentally-benign catalysts for the selective catalytic reduction of NO_x from diesel engines: Structure–activity relationship and reaction mechanism aspects. *Chem. Commun.* **2014**, *50*, 8445–8463. [[CrossRef](#)]
60. Zhan, S.; Qiu, M.; Yang, S.; Zhu, D.; Yu, H.; Li, Y. Facile preparation of MnO_2 doped Fe_2O_3 hollow nanofibers for low temperature SCR of NO with NH_3 . *J. Mater. Chem. A* **2014**, *2*, 20486–20493. [[CrossRef](#)]
61. Li, Y.; Wan, Y.; Li, Y.; Zhan, S.; Guan, Q.; Tian, Y. Low-temperature selective catalytic reduction of NO with NH_3 over Mn_2O_3 -doped Fe_2O_3 hexagonal microsheets. *ACS Appl. Mater. Interfaces* **2016**, *8*, 5224–5233. [[CrossRef](#)]
62. Yan, L.; Liu, Y.; Zha, K.; Li, H.; Shi, L.; Zhang, D. Scale-activity relationship of $\text{MnO}_x\text{-FeO}_y$ nanocage catalysts derived from prussian blue analogues for low-temperature NO reduction: Experimental and DFT studies. *ACS Appl. Mater. Interfaces* **2017**, *9*, 2581–2593. [[CrossRef](#)] [[PubMed](#)]
63. Mu, J.; Li, X.; Sun, W.; Fan, S.; Wang, X.; Wang, L.; Qin, M.; Gan, G.; Yin, Z.; Zhang, D. Inductive effect boosting catalytic performance of advanced $\text{Fe}_{1-x}\text{V}_x\text{O}_8$ catalysts in low-temperature NH_3 selective catalytic reduction: Insight into the structure, interaction, and mechanisms. *ACS Catal.* **2018**, *8*, 6760–6774. [[CrossRef](#)]
64. Li, Y.; Han, X.; Hou, Y.; Guo, Y.; Liu, Y.; Cui, Y.; Huang, Z. Role of CTAB in the improved H_2O resistance for selective catalytic reduction of NO with NH_3 over iron titanium catalyst. *Chem. Eng. J.* **2018**, *347*, 313–321. [[CrossRef](#)]
65. Qiu, M.; Zhan, S.; Yu, H.; Zhu, D. Low-temperature selective catalytic reduction of NO with NH_3 over ordered mesoporous $\text{Mn}_x\text{Co}_{3-x}\text{O}_4$ catalyst. *Catal. Commun.* **2015**, *62*, 107–111. [[CrossRef](#)]
66. Qiu, M.; Zhan, S.; Yu, H.; Zhu, D.; Wang, S. Facile preparation of ordered mesoporous MnCo_2O_4 for low-temperature selective catalytic reduction of NO with NH_3 . *Nanoscale* **2015**, *7*, 2568–2577. [[CrossRef](#)]
67. Hu, H.; Cai, S.; Li, H.; Huang, L.; Shi, L.; Zhang, D. In Situ DRIFTS investigation of the low-temperature reaction mechanism over Mn-doped Co_3O_4 for the selective catalytic reduction of NO_x with NH_3 . *J. Phys. Chem. C* **2015**, *119*, 22924–22933. [[CrossRef](#)]

68. Qiao, J.; Wang, N.; Wang, Z.; Sun, W.; Sun, K. Porous bimetallic $Mn_2Co_1O_x$ catalysts prepared by a one-step combustion method for the low temperature selective catalytic reduction of NO_x with NH_3 . *Catal. Commun.* **2015**, *72*, 111–115. [[CrossRef](#)]
69. Kang, M.; Park, E.D.; Kim, J.M.; Yie, J.E. Cu–Mn mixed oxides for low temperature NO reduction with NH_3 . *Catal. Today* **2006**, *111*, 236–241. [[CrossRef](#)]
70. Guo, R.-T.; Zhen, W.-L.; Pan, W.-G.; Zhou, Y.; Hong, J.-N.; Xu, H.-J.; Jin, Q.; Ding, C.-G.; Guo, S.-Y. Effect of Cu doping on the SCR activity of CeO_2 catalyst prepared by citric acid method. *J. Ind. Eng. Chem.* **2014**, *20*, 1577–1580. [[CrossRef](#)]
71. Ali, S.; Chen, L.; Li, Z.; Zhang, T.; Li, R.; Bakhtiar, S.U.H.; Leng, X.; Yuan, F.; Niu, X.; Zhu, Y. $Cu_x-Nb_{1.1-x}$ ($x = 0.45, 0.35, 0.25, 0.15$) bimetal oxides catalysts for the low temperature selective catalytic reduction of NO with NH_3 . *Appl. Catal. B* **2018**, *236*, 25–35. [[CrossRef](#)]
72. Yan, Q.; Chen, S.; Zhang, C.; Wang, Q.; Louis, B. Synthesis and catalytic performance of $Cu_1Mn_{0.5}Ti_{0.5}O_x$ mixed oxide as low-temperature NH_3 -SCR catalyst with enhanced SO_2 resistance. *Appl. Catal. B* **2018**, *238*, 236–247. [[CrossRef](#)]
73. Liu, J.; Li, X.; Li, R.; Zhao, Q.; Ke, J.; Xiao, H.; Wang, L.; Liu, S.; Tadé, M.; Wang, S. Facile synthesis of tube-shaped Mn-Ni-Ti solid solution and preferable Langmuir-Hinshelwood mechanism for selective catalytic reduction of NO_x by NH_3 . *Appl. Catal. A* **2018**, *549*, 289–301. [[CrossRef](#)]
74. Wang, C.; Yu, F.; Zhu, M.; Wang, X.; Dan, J.; Zhang, J.; Cao, P.; Dai, B. Microspherical $MnO_2-CeO_2-Al_2O_3$ mixed oxide for monolithic honeycomb catalyst and application in selective catalytic reduction of NO_x with NH_3 at 50–150 °C. *Chem. Eng. J.* **2018**, *346*, 182–192. [[CrossRef](#)]
75. Cheng, K.; Liu, B.; Song, W.; Liu, J.; Chen, Y.; Zhao, Z.; Wei, Y. Effect of Nb promoter on the structure and performance of iron titanate catalysts for the selective catalytic reduction of NO with NH_3 . *Ind. Eng. Chem. Res.* **2018**, *57*, 7802–7810. [[CrossRef](#)]
76. Yan, Q.; Chen, S.; Qiu, L.; Gao, Y.; O'Hare, D.; Wang, Q. The synthesis of $Cu_yMn_zAl_{1-z}O_x$ mixed oxide as a low-temperature NH_3 -SCR catalyst with enhanced catalytic performance. *Dalton Trans.* **2018**, *47*, 2992–3004. [[CrossRef](#)] [[PubMed](#)]
77. Geng, Y.; Shan, W.; Yang, S.; Liu, F. W-modified Mn–Ti mixed oxide catalyst for the selective catalytic reduction of NO with NH_3 . *Ind. Eng. Chem. Res.* **2018**, *57*, 9112–9119. [[CrossRef](#)]
78. Gao, F.; Tang, X.; Yi, H.; Li, J.; Zhao, S.; Wang, J.; Chu, C.; Li, C. Promotional mechanisms of activity and SO_2 tolerance of Co- or Ni-doped MnO_x-CeO_2 catalysts for SCR of NO_x with NH_3 at low Temperature. *Chem. Eng. J.* **2017**, *317*, 20–31. [[CrossRef](#)]
79. Xiong, Z.-B.; Hu, Q.; Liu, D.-Y.; Wu, C.; Zhou, F.; Wang, Y.-Z.; Jin, J.; Lu, C.-M. Influence of partial substitution of iron oxide by titanium oxide on the structure and activity of iron–cerium mixed oxide catalyst for selective catalytic reduction of NO_x with NH_3 . *Fuel* **2016**, *165*, 432–439. [[CrossRef](#)]
80. Wang, X.; Li, X.; Zhao, Q.; Sun, W.; Tade, M.; Liu, S. Improved activity of W-modified MnO_x-TiO_2 catalysts for the selective catalytic reduction of NO with NH_3 . *Chem. Eng. J.* **2016**, *288*, 216–222. [[CrossRef](#)]
81. Zamudio, M.A.; Russo, N.; Fino, D. Low temperature NH_3 selective catalytic reduction of NO_x over substituted $MnCr_2O_4$ spinel-oxide catalysts. *Ind. Eng. Chem. Res.* **2011**, *50*, 6668–6672. [[CrossRef](#)]
82. Zhang, T.; Qiu, F.; Chang, H.; Peng, Y.; Li, J. Novel W-modified $SnMnCeO_x$ catalyst for the selective catalytic reduction of NO_x with NH_3 . *Catal. Commun.* **2017**, *100*, 117–120. [[CrossRef](#)]
83. Ali, S.; Chen, L.; Yuan, F.; Li, R.; Zhang, T.; Bakhtiar, S.U.H.; Leng, X.; Niu, X.; Zhu, Y. Synergistic effect between copper and cerium on the performance of $Cu_x-Ce_{0.5-x}-Zr_{0.5}$ ($x = 0.1-0.5$) oxides catalysts for selective catalytic reduction of NO with ammonia. *Appl. Catal. B* **2017**, *210*, 223–234. [[CrossRef](#)]
84. Wei, Y.; Fan, H.; Wang, R. Transition metals (Co, Zr, Ti) modified iron-samarium oxide as efficient catalysts for selective catalytic reduction of NO_x at low-temperature. *Appl. Surf. Sci.* **2018**, *459*, 63–73. [[CrossRef](#)]
85. Gao, X.; Du, X.-S.; Cui, L.-W.; Fu, Y.-C.; Luo, Z.-Y.; Cen, K.-F. A Ce–Cu–Ti oxide catalyst for the selective catalytic reduction of NO with NH_3 . *Catal. Commun.* **2010**, *12*, 255–258. [[CrossRef](#)]
86. Xiong, Z.B.; Wu, C.; Hu, Q.; Wang, Y.Z.; Jin, J.; Lu, C.M.; Guo, D.X. Promotional effect of microwave hydrothermal treatment on the low-temperature NH_3 -SCR activity over iron-based catalyst. *Chem. Eng. J.* **2016**, *286*, 459–466. [[CrossRef](#)]
87. Cheng, K.; Song, W.; Cheng, Y.; Zheng, H.; Wang, L.; Liu, J.; Zhao, Z.; Wei, Y. Enhancing the low temperature NH_3 -SCR activity of $FeTiO_x$ catalysts via Cu doping: A combination of experimental and theoretical study. *RSC Adv.* **2018**, *8*, 19301–19309. [[CrossRef](#)]

88. Fang, N.; Guo, J.; Shu, S.; Luo, H.; Chu, Y.; Li, J. Enhancement of low-temperature activity and sulfur resistance of $\text{Fe}_{0.3}\text{Mn}_{0.5}\text{Zr}_{0.2}$ catalyst for NO removal by NH_3 -SCR. *Chem. Eng. J.* **2017**, *325*, 114–123. [[CrossRef](#)]
89. Guo, R.-T.; Sun, X.; Liu, J.; Pan, W.-G.; Li, M.-Y.; Liu, S.-M.; Sun, P.; Liu, S.-W. Enhancement of the NH_3 -SCR catalytic activity of MnTiO_x catalyst by the introduction of Sb. *Appl. Catal. A* **2018**, *558*, 1–8. [[CrossRef](#)]
90. Shi, J.-W.; Gao, G.; Fan, Z.; Gao, C.; Wang, B.; Wang, Y.; Li, Z.; He, C.; Niu, C. $\text{Ni}_y\text{Co}_{1-y}\text{Mn}_2\text{O}_x$ microspheres for the selective catalytic reduction of NO_x with NH_3 : The synergetic effects between Ni and Co for improving low-temperature catalytic performance. *Appl. Catal. A* **2018**, *560*, 1–11. [[CrossRef](#)]
91. Wu, X.; Feng, Y.; Du, Y.; Liu, X.; Zou, C.; Li, Z. Enhancing DeNO_x performance of CoMnAl mixed metal oxides in low-temperature NH_3 -SCR by optimizing layered double hydroxides (LDHs) precursor template. *Appl. Surf. Sci.* **2019**, *467–468*, 802–810. [[CrossRef](#)]
92. Leng, X.; Zhang, Z.; Li, Y.; Zhang, T.; Ma, S.; Yuan, F.; Niu, X.; Zhu, Y. Excellent low temperature NH_3 -SCR activity over $\text{Mn}_a\text{Ce}_{0.3}\text{TiO}_x$ ($a = 0.1–0.3$) oxides: Influence of Mn addition. *Fuel Process. Technol.* **2018**, *181*, 33–43. [[CrossRef](#)]
93. Ali, S.; Li, Y.; Zhang, T.; Bakhtiar, S.U.H.; Leng, X.; Li, Z.; Yuan, F.; Niu, X.; Zhu, Y. Promotional effects of Nb on selective catalytic reduction of NO with NH_3 over $\text{Fe}_x\text{-Nb}_{0.5-x}\text{-Ce}_{0.5}$ ($x = 0.45, 0.4, 0.35$) oxides catalysts. *Mol. Catal.* **2018**, *461*, 97–107. [[CrossRef](#)]
94. Sun, C.; Liu, H.; Chen, W.; Chen, D.; Yu, S.; Liu, A.; Dong, L.; Feng, S. Insights into the Sm/Zr co-doping effects on N_2 selectivity and SO_2 resistance of a $\text{MnO}_x\text{-TiO}_2$ catalyst for the NH_3 -SCR reaction. *Chem. Eng. J.* **2018**, *347*, 27–40. [[CrossRef](#)]
95. Yan, Q.; Chen, S.; Zhang, C.; O'Hare, D.; Wang, Q. Synthesis of $\text{Cu}_{0.5}\text{Mg}_{1.5}\text{Mn}_{0.5}\text{Al}_{0.5}\text{O}_x$ mixed oxide from layered double hydroxide precursor as highly efficient catalyst for low-temperature selective catalytic reduction of NO_x with NH_3 . *J. Colloid Interface Sci.* **2018**, *526*, 63–74. [[CrossRef](#)] [[PubMed](#)]
96. Chen, L.; Yuan, F.; Li, Z.; Niu, X.; Zhu, Y. Synergistic effect between the redox property and acidity on enhancing the low temperature NH_3 -SCR activity for NO_x removal over the $\text{Co}_{0.2}\text{Ce}_x\text{Mn}_{0.8-x}\text{Ti}_{10}$ ($x = 0–0.40$) oxides catalysts. *Chem. Eng. J.* **2018**, *354*, 393–406. [[CrossRef](#)]
97. Peña, D.A.; Uphade, B.S.; Reddy, E.P.; Smirniotis, P.G. Identification of surface species on titania-supported manganese, chromium, and copper oxide low-temperature SCR catalysts. *J. Phys. Chem. B* **2004**, *108*, 9927–9936. [[CrossRef](#)]
98. Zhuang, K.; Qiu, J.; Tang, F.; Xu, B.; Fan, Y. The structure and catalytic activity of anatase and rutile titania supported manganese oxide catalysts for selective catalytic reduction of NO by NH_3 . *Phys. Chem. Chem. Phys.* **2011**, *13*, 4463–4469. [[CrossRef](#)]
99. Boningari, T.; Pappas, D.K.; Ettireddy, P.R.; Kotrba, A.; Smirniotis, P.G. Influence of SiO_2 on M/TiO_2 ($\text{M} = \text{Cu}, \text{Mn}, \text{and Ce}$) formulations for low-temperature selective catalytic reduction of NO_x with NH_3 : Surface properties and key components in relation to the activity of NO_x reduction. *Ind. Eng. Chem. Res.* **2015**, *54*, 2261–2273. [[CrossRef](#)]
100. Sheng, Z.; Ma, D.; Yu, D.; Xiao, X.; Huang, B.; Yang, L.; Wang, S. Synthesis of novel $\text{MnO}_x@\text{TiO}_2$ core-shell nanorod catalyst for low-temperature NH_3 -selective catalytic reduction of NO_x with enhanced SO_2 tolerance. *Chin. J. Catal.* **2018**, *39*, 821–830. [[CrossRef](#)]
101. Cimino, S.; Totarella, G.; Tortorelli, M.; Lisi, L. Combined poisoning effect of K^+ and its counter-ion (Cl^- or NO_3^-) on $\text{MnO}_x/\text{TiO}_2$ catalyst during the low temperature NH_3 -SCR of NO. *Chem. Eng. J.* **2017**, *330*, 92–101. [[CrossRef](#)]
102. Fang, D.; Xie, J.; Hu, H.; Yang, H.; He, F.; Fu, Z. Identification of MnO_x species and Mn valence states in $\text{MnO}_x/\text{TiO}_2$ catalysts for low temperature SCR. *Chem. Eng. J.* **2015**, *271*, 23–30. [[CrossRef](#)]
103. Huang, J.; Huang, H.; Liu, L.; Jiang, H. Revisit the effect of manganese oxidation state on activity in low-temperature NO-SCR. *Mol. Catal.* **2018**, *446*, 49–57. [[CrossRef](#)]
104. Yang, S.; Qi, F.; Xiong, S.; Dang, H.; Liao, Y.; Wong, P.K.; Li, J. MnO_x supported on Fe–Ti spinel: A novel Mn based low temperature SCR catalyst with a high N_2 selectivity. *Appl. Catal. B* **2016**, *181*, 570–580. [[CrossRef](#)]
105. Liu, C.; Shi, J.-W.; Gao, C.; Niu, C. Manganese oxide-based catalysts for low-temperature selective catalytic reduction of NO_x with NH_3 : A review. *Appl. Catal. A* **2016**, *522*, 54–69. [[CrossRef](#)]
106. Peña, D.A.; Uphade, B.S.; Smirniotis, P.G. TiO_2 -supported metal oxide catalysts for low-temperature selective catalytic reduction of NO with NH_3 , I. Evaluation and characterization of first row transition metals. *J. Catal.* **2004**, *221*, 421–431. [[CrossRef](#)]

107. Smirniotis, P.G.; Sreekanth, P.M.; Peña, D.A.; Jenkins, R.G. Manganese oxide catalysts supported on TiO₂, Al₂O₃, and SiO₂: A comparison for low-temperature SCR of NO with NH₃. *Ind. Eng. Chem. Res.* **2006**, *45*, 6436–6443. [[CrossRef](#)]
108. Ettireddy, P.R.; Ettireddy, N.; Mamedov, S.; Boolchand, P.; Smirniotis, P.G. Surface characterization studies of TiO₂ supported manganese oxide catalysts for low temperature SCR of NO with NH₃. *Appl. Catal. B* **2007**, *76*, 123–134. [[CrossRef](#)]
109. Boningari, T.; Pappas, D.K.; Smirniotis, P.G. Metal oxide-confined interweaved titania nanotubes M/TNT (M = Mn, Cu, Ce, Fe, V, Cr, and Co) for the selective catalytic reduction of NO_x in the presence of excess oxygen. *J. Catal.* **2018**, *365*, 320–333. [[CrossRef](#)]
110. Jia, B.; Guo, J.; Luo, H.; Shu, S.; Fang, N.; Li, J. Study of NO removal and resistance to SO₂ and H₂O of MnO_x/TiO₂, MnO_x/ZrO₂ and MnO_x/ZrO₂-TiO₂. *Appl. Catal. A* **2018**, *553*, 82–90. [[CrossRef](#)]
111. Zhang, B.; Zhang, S.; Liu, B.; Shen, H.; Li, L. High N₂ selectivity in selective catalytic reduction of NO with NH₃ over Mn/Ti-Zr catalysts. *RSC Adv.* **2018**, *8*, 12733–12741. [[CrossRef](#)]
112. Han, J.; Zhang, D.; Maitarad, P.; Shi, L.; Cai, S.; Li, H.; Huang, L.; Zhang, J. Fe₂O₃ nanoparticles anchored in situ on carbon nanotubes via an ethanol-thermal strategy for the selective catalytic reduction of NO with NH₃. *Catal. Sci. Technol.* **2015**, *5*, 438–446. [[CrossRef](#)]
113. Pourkhalil, M.; Moghaddam, A.Z.; Rashidi, A.; Towfighi, J.; Mortazavi, Y. Preparation of highly active manganese oxides supported on functionalized MWNTs for low temperature NO_x reduction with NH₃. *Appl. Surf. Sci.* **2013**, *279*, 250–259. [[CrossRef](#)]
114. Pan, S.; Luo, H.; Li, L.; Wei, Z.; Huang, B. H₂O and SO₂ deactivation mechanism of MnO_x/MWCNTs for low-temperature SCR of NO_x with NH₃. *J. Mol. Catal. A* **2013**, *377*, 154–161. [[CrossRef](#)]
115. Fang, C.; Zhang, D.; Shi, L.; Gao, R.; Li, H.; Ye, L.; Zhang, J. Highly dispersed CeO₂ on carbon nanotubes for selective catalytic reduction of NO with NH₃. *Catal. Sci. Technol.* **2013**, *3*, 803–811. [[CrossRef](#)]
116. Qu, Z.; Miao, L.; Wang, H.; Fu, Q. Highly dispersed Fe₂O₃ on carbon nanotubes for low-temperature selective catalytic reduction of NO with NH₃. *Chem. Commun.* **2015**, *51*, 956–958. [[CrossRef](#)] [[PubMed](#)]
117. Bai, S.; Li, H.; Wang, L.; Guan, Y.; Jiang, S. The properties and mechanism of CuO modified carbon nanotube for NO_x removal. *Catal. Lett.* **2014**, *144*, 216–221. [[CrossRef](#)]
118. Zhang, D.; Zhang, L.; Shi, L.; Fang, C.; Li, H.; Gao, R.; Huang, L.; Zhang, J. In situ supported MnO_x-CeO_x on carbon nanotubes for the low-temperature selective catalytic reduction of NO with NH₃. *Nanoscale* **2013**, *5*, 1127–1136. [[CrossRef](#)]
119. Putluru, S.S.R.; Schill, L.; Jensen, A.D.; Siret, B.; Tabaries, F.; Fehrmann, R. Mn/TiO₂ and Mn-Fe/TiO₂ catalysts synthesized by deposition precipitation-promising for selective catalytic reduction of NO with NH₃ at low temperatures. *Appl. Catal. B* **2015**, *165*, 628–635. [[CrossRef](#)]
120. You, X.; Sheng, Z.; Yu, D.; Yang, L.; Xiao, X.; Wang, S. Influence of Mn/Ce ratio on the physicochemical properties and catalytic performance of graphene supported MnO_x-CeO₂ oxides for NH₃-SCR at low temperature. *Appl. Surf. Sci.* **2017**, *423*, 845–854. [[CrossRef](#)]
121. Fang, D.; He, F.; Liu, X.; Qi, K.; Xie, J.; Li, F.; Yu, C. Low temperature NH₃-SCR of NO over an unexpected Mn-based catalyst: Promotional effect of Mg doping. *Appl. Surf. Sci.* **2018**, *427*, 45–55. [[CrossRef](#)]
122. Lu, X.; Song, C.; Jia, S.; Tong, Z.; Tang, X.; Teng, Y. Low-temperature selective catalytic reduction of NO_x with NH₃ over cerium and manganese oxides supported on TiO₂-graphene. *Chem. Eng. J.* **2015**, *260*, 776–784. [[CrossRef](#)]
123. Wang, X.; Wu, S.; Zou, W.; Yu, S.; Gui, K.; Dong, L. Fe-Mn/Al₂O₃ catalysts for low temperature selective catalytic reduction of NO with NH₃. *Chin. J. Catal.* **2016**, *37*, 1314–1323. [[CrossRef](#)]
124. Shi, J.; Zhang, Z.; Chen, M.; Zhang, Z.; Shangguan, W. Promotion effect of tungsten and iron co-addition on the catalytic performance of MnO_x/TiO₂ for NH₃-SCR of NO_x. *Fuel* **2017**, *210*, 783–789. [[CrossRef](#)]
125. Zhao, C.; Wu, Y.; Liang, H.; Chen, X.; Tang, J.; Wang, X. N-doped graphene and TiO₂ supported manganese and cerium oxides on low-temperature selective catalytic reduction of NO_x with NH₃. *J. Adv. Ceram.* **2018**, *7*, 197–206. [[CrossRef](#)]
126. Fan, Y.; Ling, W.; Huang, B.; Dong, L.; Yu, C.; Xi, H. The synergistic effects of cerium presence in the framework and the surface resistance to SO₂ and H₂O in NH₃-SCR. *J. Ind. Eng. Chem.* **2017**, *56*, 108–119. [[CrossRef](#)]
127. Xu, Q.; Yang, W.; Cui, S.; Street, J.; Luo, Y. Sulfur resistance of Ce-Mn/TiO₂ catalysts for low-temperature NH₃-SCR. *R. Soc. Open Sci.* **2018**, *5*, 171846. [[CrossRef](#)] [[PubMed](#)]

128. Lin, L.-Y.; Lee, C.-Y.; Zhang, Y.-R.; Bai, H. Aerosol-assisted deposition of Mn-Fe oxide catalyst on TiO₂ for superior selective catalytic reduction of NO with NH₃ at low temperatures. *Catal. Commun.* **2018**, *111*, 36–41. [[CrossRef](#)]
129. Lee, T.; Bai, H. Metal Sulfate poisoning effects over MnFe/TiO₂ for selective catalytic reduction of NO by NH₃ at low temperature. *Ind. Eng. Chem. Res.* **2018**, *57*, 4848–4858. [[CrossRef](#)]
130. Mu, J.; Li, X.; Sun, W.; Fan, S.; Wang, X.; Wang, L.; Qin, M.; Gan, G.; Yin, Z.; Zhang, D. Enhancement of low-temperature catalytic activity over a highly dispersed Fe–Mn/Ti catalyst for selective catalytic reduction of NO_x with NH₃. *Ind. Eng. Chem. Res.* **2018**, *57*, 10159–10169. [[CrossRef](#)]
131. Liu, J.; Guo, R.-T.; Li, M.-Y.; Sun, P.; Liu, S.-M.; Pan, W.-G.; Liu, S.-W.; Sun, X. Enhancement of the SO₂ resistance of Mn/TiO₂ SCR catalyst by Eu modification: A mechanism study. *Fuel* **2018**, *223*, 385–393. [[CrossRef](#)]
132. Sun, P.; Huang, S.-X.; Guo, R.-T.; Li, M.-Y.; Liu, S.-M.; Pan, W.-G.; Fu, Z.-G.; Liu, S.-W.; Sun, X.; Liu, J. The enhanced SCR performance and SO₂ resistance of Mn/TiO₂ catalyst by the modification with Nb: A mechanistic study. *Appl. Surf. Sci.* **2018**, *447*, 479–488. [[CrossRef](#)]
133. Sun, X.; Guo, R.-T.; Liu, J.; Fu, Z.-G.; Liu, S.-W.; Pan, W.-G.; Shi, X.; Qin, H.; Wang, Z.-Y.; Liu, X.-Y. The enhanced SCR performance of Mn/TiO₂ catalyst by Mo modification: Identification of the promotion mechanism. *Int. J. Hydrogen Energy* **2018**, *43*, 16038–16048. [[CrossRef](#)]
134. Fan, J.; Lv, M.; Luo, W.; Ran, X.; Deng, Y.; Zhang, W.-X.; Yang, J. Exposed metal oxide active sites on mesoporous titania channels: A promising design for low-temperature selective catalytic reduction of NO with NH₃. *Chem. Commun.* **2018**, *54*, 3783–3786. [[CrossRef](#)] [[PubMed](#)]
135. Li, G.; Wang, B.; Wang, H.; Ma, J.; Xu, W.Q.; Li, Y.; Han, Y.; Sun, Q. Fe and/or Mn oxides supported on fly ash-derived SBA-15 for low-temperature NH₃-SCR. *Catal. Commun.* **2018**, *108*, 82–87. [[CrossRef](#)]
136. Li, G.; Wang, B.; Wang, Z.; Li, Z.; Sun, Q.; Xu, W.Q.; Li, Y. Reaction mechanism of low-temperature selective catalytic reduction of NO_x over Fe-Mn oxides supported on fly-ash-derived SBA-15 molecular sieves: Structure–activity relationships and in situ DRIFT analysis. *J. Phys. Chem. C* **2018**, *122*, 20210–20231. [[CrossRef](#)]
137. Tang, X.; Li, C.; Yi, H.; Wang, L.; Yu, Q.; Gao, F.; Cui, X.; Chu, C.; Li, J.; Zhang, R. Facile and fast synthesis of novel Mn₂CoO₄@rGO catalysts for the NH₃-SCR of NO_x at low temperature. *Chem. Eng. J.* **2018**, *333*, 467–476. [[CrossRef](#)]
138. Wang, C.; Zhang, C.; Zhao, Y.; Yan, X.; Cao, P. Poisoning effect of SO₂ on honeycomb cordierite-based Mn–Ce/Al₂O₃ catalysts for NO reduction with NH₃ at low temperature. *Appl. Sci.* **2018**, *8*, 95. [[CrossRef](#)]
139. Meng, H.; Liu, J.; Du, Y.; Hou, B.; Wu, X.; Xie, X. Novel Cu-based oxides catalyst from one-step carbothermal reduction decomposition method for selective catalytic reduction of NO with NH₃. *Catal. Commun.* **2019**, *119*, 101–105. [[CrossRef](#)]
140. Li, L.; Zhang, L.; Ma, K.; Zou, W.; Cao, Y.; Xiong, Y.; Tang, C.; Dong, L. Ultra-low loading of copper modified TiO₂/CeO₂ catalysts for low-temperature selective catalytic reduction of NO by NH₃. *Appl. Catal. B* **2017**, *207*, 366–375. [[CrossRef](#)]
141. Zhu, Y.; Zhang, Y.; Xiao, R.; Huang, T.; Shen, K. Novel holmium-modified Fe-Mn/TiO₂ catalysts with a broad temperature window and high sulfur dioxide tolerance for low-temperature SCR. *Catal. Commun.* **2017**, *88*, 64–67. [[CrossRef](#)]
142. Nam, K.B.; Kwon, D.W.; Hong, S.C. DRIFT study on promotion effects of tungsten-modified Mn/Ce/Ti catalysts for the SCR reaction at low-temperature. *Appl. Catal. A* **2017**, *542*, 55–62. [[CrossRef](#)]
143. Zhao, B.; Ran, R.; Guo, X.; Cao, L.; Xu, T.; Chen, Z.; Wu, X.; Si, Z.; Weng, D. Nb-modified Mn/Ce/Ti catalyst for the selective catalytic reduction of NO with NH₃ at low temperature. *Appl. Catal. A* **2017**, *545*, 64–71. [[CrossRef](#)]
144. Li, Y.; Li, G.; Lu, Y.; Hao, W.; Wei, Z.; Liu, J.; Zhang, Y. Denitrification performance of non-pitch coal-based activated coke by the introduction of MnO_x–CeO_x–M (FeO_x, CoO_x) at low temperature. *Mol. Catal.* **2018**, *445*, 21–28. [[CrossRef](#)]
145. Pan, Y.; Shen, Y.; Jin, Q.; Zhu, S. Promotional effect of Ba additives on MnCeO_x/TiO₂ catalysts for NH₃-SCR of NO at low temperature. *J. Mater. Res.* **2018**, *33*, 2414–2422. [[CrossRef](#)]
146. Wang, X.; Liu, Y.; Ying, Q.; Yao, W.; Wu, Z. The superior performance of Nb-modified Cu-Ce-Ti mixed oxides for the selective catalytic reduction of NO with NH₃ at low temperature. *Appl. Catal. A* **2018**, *562*, 19–27. [[CrossRef](#)]

147. Li, W.; Zhang, C.; Li, X.; Tan, P.; Zhou, A.; Fang, Q.; Chen, G. Ho-modified Mn–Ce/TiO₂ for low-temperature SCR of NO_x with NH₃: Evaluation and characterization. *Chin. J. Catal.* **2018**, *39*, 1653–1663. [[CrossRef](#)]
148. Lu, P.; Li, R.; Xing, Y.; Li, Y.; Zhu, T.; Yue, H.; Wu, W. Low temperature selective catalytic reduction of NO_x with NH₃ by activated coke loaded with Fe_xCo_yCe_zO_m: The enhanced activity, mechanism and kinetics. *Fuel* **2018**, *233*, 188–199. [[CrossRef](#)]
149. Zhao, X.; Mao, L.; Dong, G. Mn–Ce–V–WO_x/TiO₂ SCR catalysts: Catalytic activity, stability and interaction among catalytic oxides. *Catalysts* **2018**, *8*, 76. [[CrossRef](#)]



© 2019 by the authors. Licensee MDPI, Basel, Switzerland. This article is an open access article distributed under the terms and conditions of the Creative Commons Attribution (CC BY) license (<http://creativecommons.org/licenses/by/4.0/>).